Dawidowski, M., Król, M., Szulczyk, B., Chodkowski, A., Podsadni, P., Konopelski, P., Ufnal, M., Szuberski, P., Wróbel, M. Z., Zhang, Y., El Harchi, A., Hancox, J. C., Jarkovska, D., Mistrova, E., Sviglerova, J., Štengl, M., Popowicz, G. M., & Turło, J. (2020). Structure-activity relationship and cardiac safety of 2-aryl-2-(pyridin-2-yl)acetamides as a new class of broad-spectrum anticonvulsants derived from Disopyramide. *Bioorganic chemistry*, *98*, [103717]. https://doi.org/10.1016/j.bioorg.2020.103717

Bioorganic Chemistry 98 (2020) 103717

Contents lists available at ScienceDirect

Bioorganic Chemistry

journal homepage: www.elsevier.com/locate/bioorg

Structure-activity relationship and cardiac safety of 2-aryl-2-(pyridin-2-yl) acetamides as a new class of broad-spectrum anticonvulsants derived from Disopyramide

Maciej Dawidowski[a,*], Marek Król[a], Bartłomiej Szulczyk[a,b], Andrzej Chodkowski[a], Piotr Podsadni[a], Piotr Konopelski[c], Marcin Ufnal[c], Piotr Szuberski[a], Martyna Zofia Wróbel[a], Yihong Zhang[d], Aziza El Harchi[d], Jules C. Hancox[d], Dagmar Jarkovska[e], Eliska Mistrova[e], Jitka Sviglerova[e], Milan Štengl[e], Grzegorz M. Popowicz[f], Jadwiga Turło[a]

[a] Department of Drug Technology and Pharmaceutical Biotechnology, Medical University of Warsaw, Banacha 1, 02-097 Warsaw, Poland
[b] Laboratory of Physiology and Pathophysiology, Centre for Preclinical Research, Medical University of Warsaw, Banacha 1B, 02-097 Warsaw, Poland
[c] Department of Experimental Physiology and Pathophysiology, Centre for Preclinical Research, Medical University of Warsaw, Banacha 1B, 02-097 Warsaw, Poland
[d] School of Physiology, Pharmacology and Neuroscience, Faculty of Medical Sciences, University of Bristol, Bristol BS8 1TD, United Kingdom
[e] Department of Physiology, Biomedical Center, Faculty of Medicine in Pilsen, Charles University, Alej Svobody 1655/76, 323 00 Pilsen, Czech Republic
[f] Institute of Structural Biology, Helmholtz Zentrum München, Ingolstädter Landstrasse 1, 85764 Neuherberg, Germany

ARTICLE INFO

Keywords:
Voltage-gated sodium channel
Sodium channel blocker
Disopyramide
Drug discovery
Structure-activity relationships
Anticonvulsant agent
Refractory epilepsy
Drug repositioning
Medicinal Chemistry
Cardiac safety

ABSTRACT

A series of 2-aryl-2-(pyridin-2-yl)acetamides were synthesized and screened for their anticonvulsant activity in animal models of epilepsy. The compounds were broadly active in the 'classical' maximal electroshock seizure (MES) and subcutaneous Metrazol (scMET) tests as well as in the 6 Hz and kindling models of pharmacoresistant seizures. Furthermore, the compounds showed good therapeutic indices between anticonvulsant activity and motor impairment. Structure-activity relationship (SAR) trends clearly showed the highest activity resides in unsubstituted phenyl derivatives or compounds having *ortho*- and *meta*- substituents on the phenyl ring. The 2-aryl-2-(pyridin-2-yl)acetamides were derived by redesign of the cardiotoxic sodium channel blocker Disopyramide (DISO). Our results show that the compounds preserve the capability of the parent compound to inhibit voltage gated sodium currents in patch-clamp experiments; however, in contrast to DISO, a representative compound from the series **1** displays high levels of cardiac safety in a panel of *in vitro* and *in vivo* experiments.

1. Introduction

Epilepsy is a major neurological disorder that affects 65–70 million people globally [1]. At present, the main way of treatment of the disease is the chronic administration of Antiepileptic Drugs (AEDs) that provide symptomatic benefit by decreasing the number of seizure episodes. Since the introduction of potassium bromide in the mid-19th century, nearly 40 clinically effective AEDs have been developed. Despite the significant improvement in efficacy and safety of pharmacotherapy of epilepsy, still an adequate seizure control can be achieved in only 70% of patients. Given this failure rate and in view of physical, social and psychological consequences of uncontrolled seizures, there is a pressing need for new agents to treat refractory epilepsy.

One possible approach to the development of new AEDs leads is through structural modification of drugs that are already known to possess desirable clinical profiles. This strategy primarily leads to 'evolutionary AEDs' that display similar activity spectra but improved pharmacokinetics and safety when compared with the parent therapeutics (e.g. Oxcarbazepine, Eslicarbazepine, Fosphenytoin, Brivaracetam) [2,3].

A similar approach has been proposed, that exploits agents used in other indications, but which are known to act through potentially beneficial mechanisms of action. For example, epileptic seizures and cardiac arrhythmias share commonalities, one of which is the improper electrophysiological activity of brain neurons and cardiomyocytes, respectively [4]. A known drug, Phenytoin (PHE), exemplifies a direct use of a single chemical entity for both indications. There are other data suggesting that certain antiarrhythmic drugs (AADs) and their

* Corresponding author.
E-mail address: maciej.dawidowski@wum.edu.pl (M. Dawidowski).

https://doi.org/10.1016/j.bioorg.2020.103717
Received 2 October 2019; Received in revised form 23 December 2019; Accepted 28 February 2020
Available online 05 March 2020

derivatives are active in animal epilepsy models [4,5]; Examples are presented in Public Access to Neuroactive & Anticonvulsant Chemical Evaluations (PANAChE) database [6], a remarkable tool that provides open access to nonproprietary chemical structures and biological data for compounds previously screened in the Epilepsy Therapy Screening Program (ETSP, formerly: Anticonvulsant Screening Program, ASP) [7] of the National Institute of Neurological Disorders and Stroke (NINDS), National Institutes of Health (NIH), USA. On the other hand, direct repositioning of AADs to AEDs might bear a risk of causing severe side effects in epileptic patients. Hence, we proposed that another strategy, consisting of careful structural re-design of certain AADs might have the potential to reposition them towards management of epileptic seizures. This may be achieved through specifying those pharmacophoric features of a template AAD that would be responsible for the desired activity within the CNS and those that are expected to trigger the unwanted cardiac side-effects. Subsequently, the design strategy should be validated by chemical synthesis and a thorough pharmacological evaluation of the re-designed template.

We have chemically modified an old-generation antiarrhythmic, disopyramide (DISO), to obtain 2-aryl-2-(piridin-2-yl)acetamide, a novel scaffold for centrally acting voltage-gated Na^+ current inhibitors with a broad spectrum activity across the *in vivo* animal models of epilepsy [8]. Importantly, we have demonstrated, that a compound from the class, 2-(2-chlorophenyl)-2-(pyridin-2-yl)acetamide (**1**, ADD424042, Fig. 1A) was effective in suppressing seizures in six-hertz (6 Hz) and kindling models of pharmacoresistant epilepsy and epileptogenesis. In the present study, we present a thorough structure-antiseizure activity relationship study of 2-aryl-2-piridinylacetamide series of anticonvulsants derived from DISO.

It has been shown that there exist pathophysiological similarities between epilepsy and some forms of chronic pain and AEDs are among the important medications for this indication [9,10]. One of the physiological backgrounds by which some AEDs attenuate pain is modulation of abnormal neuronal activity by the blockade of voltage-gated Na^+ currents [11]. As this mechanism is also characteristic for 2-aryl-2-(piridin-2-yl)acetamides, in the current study we investigated whether this class of compounds is effective in a preliminary model of hyperalgesia in mice, the formalin test [12].

DISO has a relatively narrow therapeutic index and is known to produce cardiotoxicity by several possible mechanisms [13–15]. Notably, our preliminary studies in rats show that contrary to the parent DISO, the 2-aryl-2-piridinylacetamide scaffold lacked apparent cardiac side-effects in rats [8]. Here, we investigate this phenomenon in more detail, at a molecular, cellular and *in vivo* level.

2. Results and discussion

2.1. Chemistry

We systematically exploited structure–activity relationship (SAR) within 2-aryl-2-(pyridin-2-yl)acetamide series by dividing the scaffold into three subunits (Fig. 1B).

First, we varied the aromatic portion of the molecule by changing substitution patterns of the benzene ring or by replacing it with either bioisosteric pyridine or a larger, more aromatic and hydrophobic naphthalene. The planned derivatives **3a–q** (Schemes 1 and 2) were synthesized adopting the established synthetic pathway [16,17]. Briefly, the starting arylacetonitriles were deprotonated with KOH in DMSO and the resulting carboanions were C-arylated with 2-bromopyridine in a one-pot procedure. Subsequently, the obtained 2-aryl-2-pyridilacetonitriles **2a–q** were hydrolyzed to give the corresponding amides **3a–q**.

Next, we sought to investigate derivatives bearing small hydrophobic substituents (-F and $–CH_3$) onto alpha-carbon of 2-aryl-2-piridinylacetamide **3r** and **3s**. Deprotonation of **2a** with LDA, followed by methylation or electrophilic fluorination gave the respective 2-methyl- and 2-fluoro-2-phenyl-2-pyridilacetonitriles **2r** and **2s** (Scheme 3). The subsequent acidic hydrolysis provided the corresponding amides **3r** and **3s**.

Finally, by synthesizing derivatives **5a–e** we aimed to examine whether various (aryl)aliphatic residues on the amide functional group are tolerated (Scheme 4). Briefly, **2a** was subjected to Pinner reaction to give the ester **4**. The attempts to hydrolyze **4** to the corresponding carboxylic acid failed and only the decarboxylation product, 2-benzylpyridine, was detected by LC/MS analyses of the test reaction mixtures. To circumvent this issue, **4** was converted to the secondary amides **5a–e** directly, through a TBD-catalyzed aminolysis [18] with the corresponding amines.

2.2. Anticonvulsant testing

The synthesized compounds were evaluated in various *in vivo* rodent models of epilepsy within the ETSP (formerly: ASP) of NINDS, USA, according to the well-established experimental procedures and decision schemes that have been described in details in a recent article [7] and in the PANAChE database [6].

Initially, the compounds were assessed qualitatively in three rodent models of acute seizures: the MES, the scMET and the six-hertz (6 Hz) tests. The MES and scMET tests are often described as the ‘classical models’. The MES model employs an electrical stimulus to generate generalized tonic-clonic seizures and is capable of identifying the compounds that prevent seizure spread. The scMET test uses Metrazol, a chemoconvulsant, to induce myoclonic seizures and is proposed to recognize the agents raising the seizure threshold. The ‘classical’ MES and scMET models are sensitive to a wide range of marketed anticonvulsant agents, and since decades they have played an important role in discovery of new AEDs. On the other hand, they sometimes fail to identify compounds with novel mechanisms of action that are efficient in treatment of refractory epilepsy (eg. Levetiracetam, LEV)[19,20]. Therefore, another preliminary model, the six-hertz (6 Hz) test, is now routinely performed by ETSP to raise the threshold for advancing compounds for the management of pharmacoresistant seizures. The model employs an electrical current of low intensity and long duration to elicit ‘psychomotor’ seizures. The selected 2-aryl-2-(pyridin-2-yl) acetamide derivatives were tested in two variants of the 6 Hz test, at 32 and 44 mA current intensities. In those variants, different stimuli are

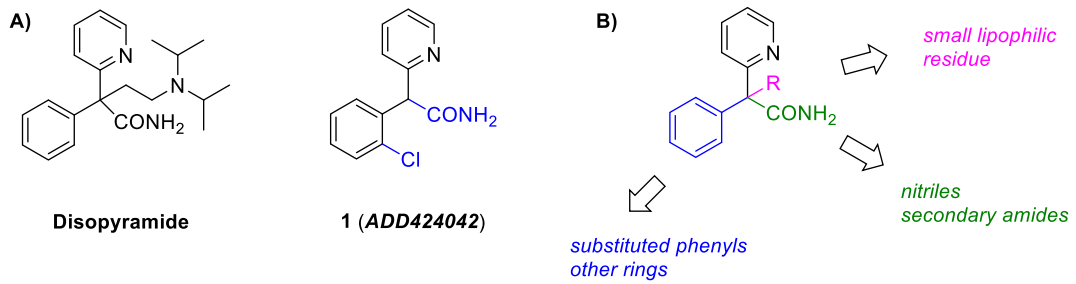

Fig. 1. (A) Chemical structures of DISO and **1**; (B) the proposed derivatization sites for the structure–activity relationship (SAR) study.

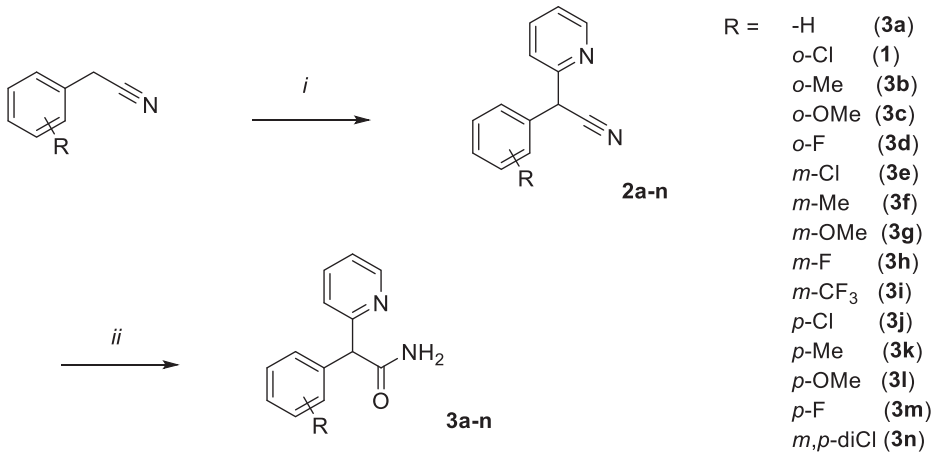

Scheme 1. *i.* 2-bromopyridine, KOH, DMSO, 60 °C; *ii.* H_2SO_4, CH_3COOH, 50 °C.

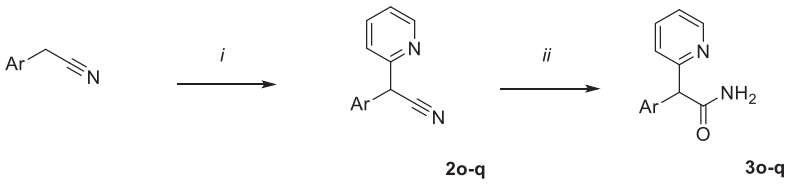

Scheme 2. *i.* 2-bromopyridine, KOH, DMSO, 60 °C; *ii.* H_2SO_4, CH_3COOH, 50 °C.

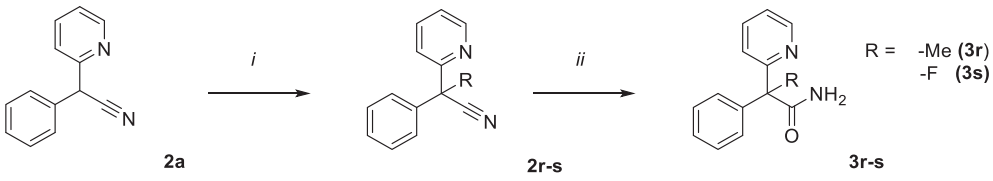

Scheme 3. *i.* LDA, THF, −78 °C, then CH_3I (**1r**) or NFSI (**1s**), −78 °C to 25 °C; *ii.* H_2SO_4, CH_3COOH, 50 °C.

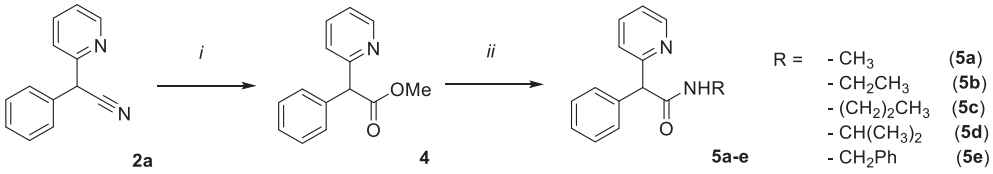

Scheme 4. *i.* HCl, MeOH, 25 °C; *ii.* RNH_2, TBD (30 mol%), THF, 60 °C.

employed for inducing seizures that are unequally susceptible to known AEDs. For example, LEV and Ethosuximide (ESM) display high efficacy in the 6 Hz test at 32 mA current intensity, while a significant loss in activity is observed when 44 mA stimuli is used in the same model. Thus, it is generally accepted that testing in both variants is useful for pre-clinical differentiation of novel investigative AEDs [19]. In addition to the primary anticonvulsant screening, the acute neurological impairment (TOX) was evaluated in the rotorod test.

The preliminary screening was performed using small (1–8) groups of animals per at least one dose of the test compound, at more than one time point after its administration. The compounds showing activity in the primary MES, scMET, 6 Hz (32 and 44 mA) and TOX tests were subsequently quantified to determine the median effective doses (ED_{50}), toxic doses (TD_{50}) and protective indices (PI = TD_{50}/ED_{50}) at the previously estimated time of peak effects (TPEs). The experimental ED_{50}, TD_{50} and PI values were then compared with those of reference AEDs. Finally, according to ETSP dispositions, selected agents were chosen for screening in the Corneal Kindled Mouse (CKM) model and Lamotrigine (LTG)-Resistant Amygdala Kindled Rat model of pharmacoresistant, complex partial seizures. The results of the aforementioned tests are summarized in Tables 1–8 and S1–5.

Most of the synthesized compounds showed anticonvulsant activity and moderate neurological toxicity in the preliminary MES and TOX screening, respectively, after i.p. administration in mice (Table 1). Analyzing the influence of the phenyl substitution pattern, we observed a general trend that the highest anticonvulsant activity and lowest neurotoxicity resides in the *ortho*- and *meta*-derivatives, whereas their *para*- counterparts are significantly less efficient. Notable exceptions to this tendency were 4–Cl and 4–F derivatives **3j** and **3 m**, respectively, both providing seizure protection at a dose of 100 mg/kg, 0.5 h post-administration. Nevertheless, both compounds were inactive at later time points, and, similar to all other *para*-derivatives, they produced pronounced neurotoxicity and mortality at a higher dose of 300 mg/kg. Another general observation was the loss of antiseizure efficacy of –OMe derivatives, only the *o*-OMe substituted compound **3c** showed activity, albeit it was more pronounced at dose of 300 mg/kg, at which neurotoxicity occurred. Derivative **3a**, lacking substituents in the benzene ring, displayed full seizure protection, at 100 mg/kg, 0.5 h post-administration. We did not observe acute toxic effects or motor impairment at this dose. Mortality occurred at a significantly higher dose of 300 mg/kg, still, preliminary screening indicated that a reasonable therapeutic window could be expected for the compound in the quantification studies. An important observation was that besides **3d**, a derivative of **3a** containing a fluorine atom in the benzene ring, the *ortho*-substituted compounds did not cause animal death even at a dose of 300 mg/kg, indicating good margins of tolerability and safety. On the

Table 1
Anticonvulsant activity and neurotoxicity of compounds in the MES model following intraperitoneal (ip.) administration in mice.

Compound	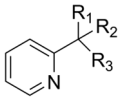			Dose (mg/kg)	MES[a]			TOX[b]		
	R_1	R_2	R_3		0.5 h	2.0 h	4.0 h	0.5 h	2.0 h	4.0 h
1	*o*-ClPh-	$CONH_2$	H	100	**3/3**	–[c]	**2/3**	0/8	–	0/4
				300	**1/1**	–	**1/1**	0/4	–	0/2
2a	Ph-	CN	H	100	**4/4**	**2/4**	–	0/8	0/8	–
				300	**4/4**	–	–	**8/8**	**8/8**[d]	–
2d	*o*-FPh-	CN	H	100	**4/4**	**4/4**	**1/4**	**1/8**[e]	**1/8**	0/8
3a	Ph-	$CONH_2$	H	100	**3/3**	–	0/3	0/8	–	0/8
				300	–	–	–	**4/4**[f]	–	–
3b	*o*-MePh-	$CONH_2$	H	100	**3/3**	–	**2/3**	0/8	–	0/4
				300	**1/1**	–	**1/1**	**2/8**	–	0/2
3c	*o*-OMePh-	$CONH_2$	H	100	**1/3**	–	**1/3**	0/8	–	0/8
				300	**1/1**	–	0/1	**3/4**	–	0/2
3d	*o*-FPh-	$CONH_2$	H	100	**3/3**	–	0/3	0/8	–	0/4
				300	**1/1**	–	–	**3/4**[e]	–	0/1
3e	*m*-ClPh-	$CONH_2$	H	100	**4/4**	0/4[g]	0/4	0/8	0/8	0/8
3f	*m*-MePh-	$CONH_2$	H	100	**1/4**	0/4[g]	0/4	0/8	0/8	0/8
3g	*m*-OMePh-	$CONH_2$	H	100	0/3	–	0/3	0/8	–	0/4
3h	*m*-FPh-	$CONH_2$	H	100	–	–	–	–	–	–
3i	*m*-CF_3Ph-	$CONH_2$	H	100	**4/4**	0/4[h]	0/4	**2/8**	0/8	0/8
3j	*p*-ClPh-	$CONH_2$	H	100	**2/3**	–	0/3	0/8	–	0/4
				300	**1/1**	–	–	**3/4**[i]	–	–
3k	*p*-MePh-	$CONH_2$	H	100	0/3	–	0/3	0/8	–	0/4
				300	0/1	–	–	**2/4**[e]	–	0/1
3l	*p*-OMePh-	$CONH_2$	H	100	0/3	–	0/3	0/8	–	0/4
				300	–	–	–	**3/4**[i]	–	0/0
3m	*p*-FPh-	$CONH_2$	H	100	**2/3**	–	0/3	0/8	–	0/4
				300	–	–	–	**4/4**[f]	–	–
3n	*m,p*-diClPh-	$CONH_2$	H	100	**2/3**	–	0/3	0/8	–	0/4
				300	**1/1**	–	**1/1**	0/4	–	0/2
3o	2-pyridinyl-	$CONH_2$	H	100	0/4	0/4	–	0/8	0/8	–
				300	0/4	0/4	–	**1/8**	**1/8**	–
3p	1-naphthyl-	$CONH_2$	H	100	**3/4**	0/4	–	0/8	0/8	–
				300	**4/4**	**1/4**	–	**8/8**	0/8	–
3q	2-naphthyl-	$CONH_2$	H	100	**1/4**	**2/4**	–	0/8	0/8	–
				300	**4/4**	**4/4**	–	**1/8**	0/8	–
3r	Ph-	$CONH_2$	Me	100	**4/4**	**1/4**	–	0/8	0/8	–
				300	**4/4**	**4/4**	–	**8/8**	**6/8**	–
3s	Ph-	$CONH_2$	F	100	**4/4**	**4/4**	–	**2/8**	**1/8**	–
				300	**4/4**	**4/4**	–	**8/8**	**8/8**	–
4	Ph-	COOMe	H	100	0/4	0/4	–	0/8	0/8	–
				300	**1/4**	0/4	–	0/8	0/8	–
5a	Ph-	CONHMe	H	100	0/4	**2/4**	–	0/8	0/8	–
				300	**4/4**	**4/4**	–	**1/8**	0/8	–
5b	Ph-	CONHEt	H	100	**4/4**	**4/4**	–	0/8	0/8	–
				300	**4/4**	**4/4**	–	0/8	0/8	–
5c	Ph-	CONH*n*Pr	H	100	**2/4**	**1/4**	–	0/8	0/8	–
				300	**4/4**	**4/4**	–	**8/8**	**7/8**	–
5d	Ph-	CONH*i*Pr	H	100	**1/4**	**2/4**	–	0/8	0/8	–
				300	**4/4**	**4/4**	–	**7/8**	**1/8**	–
5e	Ph-	CONHBn	H	100	**1/4**	0/4	–	0/8	0/8	–
				300	**4/4**	**4/4**	–	0/8	0/8	–

Ratios where at least one animal was protected or displayed neurotoxicity have been highlighted in bold for easier data interpretation.
[a] Maximal Electroshock test (number of animals protected/number of animals tested).
[b] Neurotoxicity test (number of animals exhibiting neurological toxicity/number of animals tested).
[c] Not determined.
[d] 6 animals died.
[e] 1 animal died
[f] 4 animals died.
[g] Active in 3/4, 1.0 h post administration.
[h] Continuous seizure activity.
[i] 3 animals died.

contrary, *para*- derivatives that lacked anticonvulsant activity in the MES model elicited high rates of mortality at the same time.

Replacement of the phenyl moiety of **3a** with 2-pyridinyl resulted in **3o**, which lacked activity. On the contrary, more bulky and hydrophobic 1- and 2-naphthalenes **3p** and **3q**, respectively, were tolerated in the MES model.

Introduction of small –Me and –F substituents at the alpha-carbon of **3a** produced corresponding **3r** and **3s** that were active in the preliminary MES screening and produced pronounced motor impairment in the initial TOX testing.

Table 2
Quantification studies of selected compounds in the MES, scMET and neurotoxicity tests in mice.

Compound	ED_{50} MES[a] (mg/kg)	ED_{50} scMET[b] (mg/kg)	TD_{50}[c] (mg/kg)	PI[d]	TPE[e] (h)
1[f]	48 (38–58)	> 270	270 (252–266)	5.6	1.0
	61 (51–72)[g]	–[h]	–	–	0.25
	56 (51–61)[i]	292 (224–366)	> 500	> 8.9	1.0
2a	85 (66–114)	107 (86–144)	156 (134–167)	1.8	0.5
2d	60 (53–67)	59 (47–73)	168 (148–195)	2.8	0.25
3a	41 (34–45)	140 (115–165)	198 (180–224)	4.8	0.25
	45 (36–57)[g]	–	166 (159–178)	3.7	0.25
	58 (44–72)[i]	160 (119–212)	> 500	> 8.6	0.25
3b	40 (32–47)	> 190	196 (170–240)	4.9	0.25
3d	43 (38–50)	132 (105–164)	207 (182–235)	4.8	0.25
3e	45 (40–50)	127 (115–139)	148 (139–164)	3.3	0.25
3i	48 (38–64)	113 (101–124)	183 (162–216)	3.8	0.25
3q	81 (70–93)	261 (209–329)	–	–	0.25
3r[i]	76 (66–85)	196 (125–282)	> 500	> 6.6	2.0
3s[i]	44 (36–52)	174 (119–227)	417 (339–488)	9.5	0.5
Carbamazepine[j]	17 (14–21)	> 45	41 (36–47)	2.4	0.25
	18 (16–28)[i]	122 (108–146)	136 (117–157)	7.6	0.5
Phenytoin[j]	7 (5–8)	> 50	51 (47–54)	7.3	1.0
	8 (7–9)[i]	> 90	89 (80–99)	11.1	4.0
Lamotrigine[k]	7 (6–9)	> 40	30 (25–36)	4.3	1.0
Lacosamide[l]	4.5 (3.7–5.5)	> 25	27 (26–28)	6.0	0.5

Unless otherwise stated, the compounds were administered i.p. in male mice. Values in parentheses are 95% confidence intervals determined by probit analysis.
[a] Maximal Electroshock test.
[b] Subcutaneous Metrazol test.
[c] ED_{50} for the neurotoxicity test.
[d] Protective index (TD_{50}/ED_{50} MES).
[e] Time to peak effect for the MES test.
[f] Data from Ref. [8].
[g] Tested in female mice.
[h] Not tested.
[i] Oral administration of the test compound.
[j] Data from PANAChE database [1,6].
[k] Data from Ref. [19].
[l] Data from Ref. [34].

Table 3
Quantification studies of selected compounds in the MES, scMET and neurotoxicity tests in rats.

Compound	ED_{50} MES[a] (mg/kg)	ED_{50} scMET[b] (mg/kg)	TD_{50}[c] (mg/kg)	PI[d]	TPE[e] (h)
1[f]	33 (23–43)	82 (57–101)	175 (162–186)	5.3	0.25
	27 (16–49)[g]	> 250	> 500	> 18.5	2.0
2a	14 (7–23)	–[h]	207 (158–284)	14.8	2.0
2d	34 (22–50)	34 (27–40)	103 (78–152)	3.0	0.5
3a	35 (25–49)	51 (36–69)	150 (104–200)	4.3	0.5
3b	16 (10–24)	> 125	139 (117–168)	8.7	0.25
3d	23 (19–27)	73 (34–114)	144 (114–166)	6.3	0.5
3i	28 (19–38)	–	158 (123–201)	5.6	0.25
	41 (25–69)[g]	> 250	> 500	> 12.2	0.25
3*n*	91 (66–122)	–	> 250	> 2.7	0.5
	45 (31–68)[g]	> 250	> 500	> 11.1	2.0
Carbamazepine[i]	4 (3–6)	> 35	34 (28–45)	> 8.5	0.25
	5 (3–8)[g]	> 250	365 (223–500)	73.0	1.0
Phenytoin[i]	2 (1–4)	> 100	15 (12–19)	6.4	0.25
	28 (20–35)[g]	> 500	> 1000	> 35.7	2.0

Unless otherwise stated, the compounds were administered i.p. Values in parentheses are 95% confidence intervals determined by probit analysis.
[a] Maximal Electroshock test.
[b] Subcutaneous Metrazol test.
[c] ED_{50} for the neurotoxicity test.
[d] Protective index (TD_{50}/ED_{50} MES).
[e] Time to peak effect.
[f] Data from Ref. [8].
[g] Oral administration of the test compound.
[h] Not tested.
[i] Data from PANAChE database.

Table 4
Effects of selected compounds on the threshold for minimal seizures induced by the timed intravenous infusion of Metrazol (MET) in mice.

Compound	Dose (mg/kg)	MET[a] (mg/kg ± S.E.M.)	
		First twitch	Clonus
1[b]	0	27.1 ± 1.21	29.3 ± 1.29
	48	32.1 ± 1.48[c]	38.8 ± 3.05[c]
	270	51.6 ± 2.98[c]	62.4 ± 3.56[c]
2d	0	32.5 ± 1.22	35.9 ± 1.47
	29	36.1 ± 1.26[d]	39.6 ± 2.09[e]
	168	73.3 ± 2.39[c]	112.6 ± 6.61[c]
3a	0	27.2 ± 1.27	29.3 ± 1.46
	41	38.6 ± 1.64[c]	46.5 ± 2.95[c]
	198	59.8 ± 1.20[c]	84.2 ± 3.71[c]
3d	0	26.1 ± 0.89	28.4 ± 1.05
	43	32.6 ± 0.93[c]	35.9 ± 0.84[c]
	207	55.2 ± 2.96[c]	72.6 ± 3.01[c]
Carbamazepine[f]	0	30.7 ± 1.03	36.9 ± 1.46
	11	31.0 ± 1.45[e]	37.5 ± 1.29[e]
	43	33.0 ± 1.04[e]	43.1 ± 2.13[d]
Phenytoin[f]	0	33.8 ± 0.95	28.4 ± 1.05
	6	33.5 ± 1.05[e]	39.7 ± 1.33[e]
	41	27.1 ± 1.48[c]	33.4 ± 1.28[c]
Mexiletin[f]	0	35.2 ± 0.59	39.8 ± 1.17
	10	32.5 ± 0.85[c]	37.3 ± 1.02[e]
	30	28.6 ± 1.19[c]	32.0 ± 1.65[c]
Valproate[f]	0	33.1 ± 1.32	38.3 ± 1.55
	263	48.8 ± 2.77[c]	66.5 ± 6.91[c]
	340	49.3 ± 3.39[c]	92.7 ± 11.72[c]

Data are expressed as means ± S.E.M.
[a] Intravenous Metrazol Seizure Threshold test.
[b] Data from Ref. [8].
[c] $p < 0.01$, Dunnett's test.
[d] $p < 0.05$, Dunnett's test.
[e] $p > 0.05$, Dunnett's test.
[f] Data from PANAChE database [1,6].

Table 5
Quantification studies of selected compounds in the 6 Hz (32 mA) and neurotoxicity tests following intraperitoneal (i.p.) administration in mice.

Compound	ED_{50} 6 Hz[a] (mg/kg)	TD_{50}[b] (mg/kg)	PI[c] 6 Hz	TPE[d] (h)
1[e]	67 (58–75)	270 (252–266)	4.0	1.0
2d	29 (19–42)	168 (148–195)	5.8	0.25
3a	20 (9–49)	184 (75–300)	9.2	0.25
3b	65 (45–83)	196 (170 – 240)	3.0	0.25
3d	34 (25–43)	207 (182–235)	6.0	0.5
3i	69 (66–72)	183 (162–216)	2.7	0.5
Carbamazepine[f]	24 (18–26)	45 (43–47)	1.9	0.25
Phenytoin[f]	> 60	51 (47–54)	< 1.0	2.0
Lamotrigine[g]	> 60	30 (25–36)	< 1.0	1.0
Lacosamide[h]	10 (8–13)	27 (26–28)	2.7	0.5
Levetiracetam[g]	19 (10–36)	> 500	> 26.3	1.0

Values in parentheses are 95% confidence intervals determined by probit analysis.
[a] 6 Hz test at 32 mA.
[b] ED_{50} for the neurotoxicity test.
[c] Protective index (TD_{50}/ED_{50} 6 Hz).
[d] Time to peak effect for the 6 Hz test.
[e] Data from Ref. [8]
[f] Data from PANAChE database [1,6].
[g] Data from Ref. [19].
[h] Data from Ref. [34].

Switching the primary amide in **3a** to nitrile resulted in **2a** that was equally efficient to the parent compound, whereas ester **4** was devoid of *in vivo* activity. Modifications consisting in substitution of the primary amide by small alkyl moieties led to **5a–e** that were effective in primary MES screening in mice. However, except for ethylamide **5b**, that

Table 6
Quantification studies of selected compounds in the 6 Hz (44 mA) and neurotoxicity tests in mice.

Compound	ED_{50} 6 Hz[a] (mg/kg)	TD_{50}[b] (mg/kg)	PI[c] 6 Hz	TPE[d] (h)
1[e]	82 (75–89)	270 (252–266)	3.3	0.5
	104 (87–126)[f]	> 500[f]	> 4.8	1.0
2d	47 (42–52)	168 (148–195)	3.6	0.25
3a	78 (55–110)	184 (75–300)	2.4	0.25
	100 (82–118)[f]	> 500[f]	> 5.0	0.5
	72 (63–80)[g]	166 (159–178)[g]	2.3	0.25
3i	75 (55–93)	183 (162–216)	2.4	0.25
3p	77 (65–94)	138 (101–191)	1.8	0.25
3r	96 (84–108)[f]	> 500[f]	> 5.2	0.5
3 s	47 (40–85)	145 (130–166)	3.1	0.5
5b	163 (103–220)	305 (276–317)	1.9	1.0
Carbamazepine[h]	34 (28–37)	45 (43–47)	1.3	0.25
Phenytoin[i]	> 60	51 (47–54)	< 1.0	2.0
Lamotrigine[i]	> 60	30 (25–36)	< 1.0	1.0
Lacosamide[j]	13 (10–18)	27 (26–28)	2.1	0.5
Levetiracetam[i]	1089 (787–2650)	> 500	> 0.5	1.0

Unless otherwise stated, the compounds were administered i.p. in male mice. Values in parentheses are 95% confidence intervals determined by probit analysis.
[a] 6 Hz test at 44 mA.
[b] ED_{50} for the neurotoxicity test
[c] Protective index (TD_{50}/ED_{50} 6 Hz).
[d] Time to peak effect for the 6 Hz test.
[e] Data from Ref. [8].
[f] The compound was administered orally (po.).
[g] Tested in female mice.
[h] Data from PANAChE database [1,6].
[i] Data from Ref. [19].
[j] Data from Ref. [35].

Table 7
Quantification studies of selected compounds in the Corneal Kindled Mouse model after intraperitoneal (i.p.) administration in mice.

Compound	ED_{50} CKM[a] (mg/kg)	TPE[b] (h)
1[c]	59 (38–83)	0.5
3a	53 (33–96)	0.25
3i	62 (45–87)	0.25
Carbamazepine[d]	9 (5–11)	0.5
Valproate[e]	174 (136–208)	0.25
Levetiracetam[d]	16 (6–43)	0.5

Values in parentheses are 95% confidence intervals determined by probit analysis.
[a] Corneal Kindled Seizure model.
[b] Time to peak effect.
[c] Data from Ref. [8].
[d] Data from Ref. [36].
[e] Data from PANAChE database [1,6].

Table 8
Quantification study of **3a** in the Lamotrigine (LTG)-Resistant Amygdala Kindled Rat model after intraperitoneal (i.p.) administration in rat.

Compound	ED_{50} LTGK[a] (mg/kg)	Time of test (h)
3a	50 (37–67)	0.5
Felbamate[b]	169 (131–206)	1.5

Values in parentheses are 95% confidence intervals determined by probit analysis.
[a] Lamotrigine (LTG) Resistant Amygdala Kindled Seizure model.
[b] Data from Ref. [21].

produced full seizure protection at 100 mg/kg, the activities of amide nitrogen-substituted derivatives were more pronounced at a relatively high dose of 300 mg/kg.

Compounds **2a**,**d** and **3a–n** were screened in the preliminary scMET screening in mice. Only **2d** showed appreciable activity (Table S1), hence, according to ETSP dispositions, the primary screening in this model was not performed for the remaining compounds.

The selected derivatives showing high activity in the preliminary screening in mice (**2a**,**d**, **3a**,**b**,**d**,**e**,**i**,**q**,**r**,**s**), were tested quantitatively in the MES, scMET and TOX models (Table 2). The ED_{50} values in the MES quantification studies after i.p. administration in male mice were roughly comparable for most compounds (ED_{50} = 40–48 mg/kg), only the nitriles **2a**,**b** and the naphthyl derivative **3q** were slightly less active (ED_{50} = 85, 60 and 81, respectively). Propitiously, the TD_{50} values in the TOX test (TD_{50} = 148–270 mg/kg) indicated satisfactory PIs (PI ~ 5 for most compounds) for the MES model. As expected on the basis of preliminary screens, the potency of the compounds in the scMET test was markedly lower than in the MES model, with ED_{50} almost reaching the TD_{50} values. A notable exception from this trend was the nitrile **2d**, which exhibited a high anticonvulsant activity and fair safety margins (ED_{50} = 59 mg/kg, PI = 2.8 for this model). In addition to the standard male mice quantification, **1** and **3a** were tested in female mice. We did not observe considerable differences in MES and TOX activities in both sexes. Selected compounds were evaluated quantitatively using oral route of administration. The anticonvulsant activities did not differ markedly as compared to the i.p. delivery. However, we observed a significant decrease in motor impairment, giving rise to higher PI values.

It has been shown in the past that seizures evoked in various rodent species are unequally susceptible to treatment with AEDs and that this feature can be useful for differentiation of novel investigative AEDs [6]. Therefore, according to ETSP dispositions, selected compounds showing activity in preliminary MES mice screening were additionally tested in rats. The qualitative results (Tables S2–S3) follow the similar SAR patterns for both rodent species. However, we observed a generally greater sensitivity of rats to antiseizure effects produced by administration of the compounds, when compared to mice. Quantification studies were performed for the selected compounds active in the qualitative rat screening (**2a**,**d**, **3a**,**b**,**d**,**i**,**n**). The results show that the ED_{50} values in the MES were lower for most of the tested agents (ED_{50} = 14–35 mg/kg) than those obtained in the similar mice study, nitrile **2a** and *ortho*-CH_3 derivative **3b** being most potent (ED_{50} = 14 and 16 mg/kg, respectively) in this model (Table 3). As a result, the PI values for the MES test were considerably better (PI = 3.0–14.8) when compared to mice results. Quantification results of the compounds in the scMET model show a similar trend, the estimated ED_{50} values being up to three-fold lower than those obtained from the corresponding mice experiments. **1**, **3i**,**n** were quantified using oral dosage. In analogy to what we had observed in the mice experiment, the anticonvulsant activity in the MES model did not depend greatly on the way of administration and a marked loss of motor impairment occurred, as judged by the TOX test. However, other than in mice, the oral administration of compounds in rats ceased their effectiveness in the scMET model completely.

Comparison of the potency of the investigated compounds in the 'classical' MES and scMET models with activities of marketed "old"-(PHE and Carbamazepine, CBZ) and "new"-generation (LTG and Lacosamide, LAC) anticonvulsant sodium channel blockers leads to several conclusions. First, the ED_{50} values of arylacetamide derivatives in the MES test are markedly lower than those of the aforementioned reference AEDs. On the other hand, both display similar PI values, suggesting the investigated arylacetamides may still have potential to be clinically useful. Noteworthy, upon variation of basic experimental conditions (ie. rodent species and routes of administration), the investigated compounds follow same qualitative changes in the activity patterns as the reference AEDs. Importantly, other than the reference 'classical' sodium channel blockers, the agents investigated here do exhibit activity in the scMET model, which could be regarded a useful feature in their further preclinical development.

As an extension of the investigations in the scMET model, **1**, **2d**, **3a**,**d** were assayed in a more discriminative timed i.v. infusion of MET (ivMET) test in mice (Table 4). This model is used to differentiate those agents that lower the seizure threshold and, as such, may be proconvulsant, from those compounds that elevate seizure threshold, and are thus anticonvulsant. The results show, that contrary to the 'classical' sodium channel blockers, and, similarly to mechanistically unrelated Valproic Acid (VPA), all tested arylacetamide derivatives significantly and dose-dependently increased the length in time to first twitch and sustained clonus following timed infusion of the convulsant MET.

The selected compounds were further tested in two variants of the 6 Hz test: at 32 and 44 mA current intensities, after intraperitoneal administration in mice. The results of the initial qualitative screening closely followed the SAR patterns previously observed during the primary assessments in the MES model (Tables S4–S5). When evaluated quantitatively using a 32 mA stimuli, **1**, **2d**, **3a**,**b**,**d**,**i** displayed high seizure-suppressing efficacy (ED_{50} = 20–69 mg/kg) and favorable safety margins (PI = 2.7–9.2, Table 5). *Ortho*-F nitrile **2d** and unsubstituted phenyl **3a** derivatives were most active in the series (ED_{50} = 29 and 20 mg/kg; PI = 5.8 and 9.2, respectively). Increasing the current intensity to 44 mA resulted in a slight drop of the anticonvulsant potency of most of the tested compounds **1**, **2d**, **3a**,**i**,**p**,**r**,**s**, **5b** (ED_{50} = 47–82 mg/kg) and narrower safety indices (PI = 1.8–3.6, Table 6). Similar to what we had observed during the quantification studies in MES model, differentiation experiments in female mice performed for **3a** did not reveal significant changes in activity in 6 Hz test. Likewise, the change in route of administration to oral greatly diminished levels of motor impairment produced by ADD424042 and **3a**.

The significant activity of phenylacetamides in the 6 Hz model is an important characteristic that differentiates them from 'classical' and newer anticonvulsant sodium channel blockers - CBZ, PHT and LTG. Further, though most of the investigated were less potent than LAC in terms of ED_{50} values comparison, they revealed favorable (at 32 mA stimuli) or at least similar (at 44 mA current intensities) PI values. Finally, some of the phenylacetamide derivatives displayed ED_{50} values comparable with mechanistically unrelated Levetiracetam (LEV) when evaluated at 32 mA and outcompeted LEV in assays employing 44 mA current intensities.

According to ETSP dispositions, compounds **3a** and **3i** were further evaluated in the CKM model of complex partial seizures (Table 7). Their ED_{50} values closely matched the one reported by us [8] for **1** and were in the ranges of potencies of CBZ, VPA and LEV used as reference AEDs.

We have recently demonstrated that **1** suppressed kindling development, when assayed qualitatively in the LTG-Resistant Amygdala Kindled Seizure (LKR) model of pharmacoresistant seizures and epileptogenesis in rats [8]. In the current study, **3a** was subjected to quantitative evaluations in this model (Table 8). The compound displayed efficacy that surpassed this of Felbamate (FEB)[21], taken as the reference AED. The activity of arylacetamides in the LKR model is another important characteristics that distinguishes them from 'classical' anticonvulsant sodium channel blockers, such as CBZ [22].

2.3. Analgesic properties in the formalin test in mice

Many of the marketed AEDs, including 'old' and 'new-generation' sodium channel blockers, are effective in treatment of pain. Thus, in the present study the selected arylacetamide derivatives were screened by ETSP in the formalin test, which is a preliminary model of acute and inflammatory pain. The compounds were tested after intraperitoneal (i.p) administration in mice, at doses corresponding to their ED_{50} values in the MES test (Table 9).

None of the tested derivatives **1**, **3a**,**b**,**d**,**m** were efficient in alleviating acute phase of pain in a statistically significant manner. On the

Table 9
Activity of selected compounds in the formalin model of hyperalgesia after intraperitoneal (i.p.) administration in mice.

Compound	Dose (mg/kg)	% of control	
		Acute phase	Inflammatory phase
1	48	79 ± 17%[a]	73 ± 15%[a]
3a	41	66 ± 16%[a]	56 ± 11%[b]
3b	40	69 ± 13%[a]	32 ± 14%[b]
3d	43	94 ± 17%[a]	118 ± 15%[a]
3m	52	85 ± 11%[a]	94 ± 23%[a]
Carbamazepine[c]	10	78 ± 17%[a]	74 ± 29%[a]
	36	49 ± 5%[d]	36 ± 19%[d]
Phenytoin[c]	6	66 ± 21%[a]	20 ± 5%[d]
Valproate[c]	100	74 ± 5%[b]	48 ± 4%[d]
	300	41 ± 6%[d]	20 ± 6%[d]

Data are expressed as means ± S.E.M.
[a] n = 8, p > 0.05 *vs* control group, Student's *t*-test.
[b] n = 8, p < 0.05 *vs* control group, Student's *t*-test.
[c] Data from PANAChE database.
[d] n = 8, p < 0.01 *vs* control group, Student's *t*-test

other hand, **3a** and **3b** attenuated the inflammatory phase in a manner similar to the reference CBZ, PHE and VPA. Overall, they showed similar profile to CBZ in this model, justifying further investigations of their possible anti-pain properties.

2.4. Inhibition of voltage-gated sodium currents

We have shown that **1** is a potent sodium channel blocker in a whole-cell patch-clamp experiment [8]. To further validate this mechanism of anticonvulsant action, we investigated the influence of a broader set of arylacetamide derivatives on voltage-gated sodium channels (Table 10). Maximal sodium currents were evoked using rectangular voltage-steps from the holding potential of −65 mV. We established previously that at this holding potential sodium currents are more sensitive to **1** as compared to −90 mV [8]. Maximal sodium currents were recorded in control and in the presence of a tested compound in a fixed concentration of 1 μM. Even at the relatively low concentration, all of the tested compounds significantly inhibited sodium currents, except **5e**, which exerted a statistically insignificant effect. Although **1**, **3a**,**b**,**s** have a similar anticonvulsant profiles and potencies in the *in vivo* epilepsy models, they produced notably unequal inhibition of maximal amplitudes of sodium currents (62 ± 3%, 56 ± 5%, 84 ± 5%, 80 ± 6%) at the tested concentration. One explanation of this would be the possible differences in their ADME/PK characteristics. On the other hand, the existence of another mechanism of action that contributes to the compounds' *in vivo* anticonvulsant activity cannot be ruled out. Importantly, **5e** inhibited sodium currents significantly more weakly than **3a** (88 ± 8% *vs* 56 ± 5%, respectively, Fig. 2, p < 0.05), which is in agreement with their unequal potencies in the primary anticonvulsant testing. In addition, we found that the parent DISO shares the same potency of blocking neuronal sodium currents as the anticonvulsant arylacetamides. We have previously reported that administration of this drug does not produce *in vivo* antiseizure effects in mice, which could result from different tissue distribution caused by the presence of the dialkylamino chain [8].

Table 10
Influence of the selected compounds (1 μM) on averaged, normalized maximal amplitudes of sodium currents in rat prefrontal cortex pyramidal neurons, evoked from a holding potential of −65 mV.

Compound	% inhibition[a]
1[b]	62 ± 3%
DISO[c]	80 ± 3%
3a[b]	56 ± 5%
3b[d]	84 ± 5%
3s[d]	80 ± 6%
5e[e]	88 ± 8%

[a] Data are expressed as means ± S.E.M.
[b] n = 5, p < 0.01, one-way ANOVA followed by the Dunnett's post hoc test.
[c] n = 4, p < 0.05, one-way ANOVA followed by the Dunnett's post hoc test.
[d] n = 5, p < 0.05, one-way ANOVA followed by the Dunnett's post hoc test.
[e] n = 6, p > 0.05, one-way ANOVA followed by the Dunnett's post hoc test.

2.5. In vitro and in vivo cardiac safety.

Clinical use of DISO is associated with some incidence of acquired long QT syndrome and torsades de pointes arrhythmia [23–25] and the drug has been established to be an inhibitor of the human Ether-à-go-go-Related Gene (hERG) potassium channels, which mediate repolarizing "I_{Kr}" potassium current, at clinically relevant concentrations [13,26].We have shown that in a contrast to DISO, a representative 2-aryl-2-(piridin-2-yl)acetamide **1** produced no apparent cardiotoxic effects in rats [8], although this species does not rely on hERG for ventricular repolarization. Therefore, in order to fully evaluate the risk of potential hERG-related cardiotoxicity of 2-aryl-2-(piridin-2-yacetamides), in the present study **1** and DISO were applied to hERG-expressing HEK293 cells and hERG current (I_{hERG}) was measured under whole-cell voltage clamp, using the protocol shown in Fig. 3A. At a concentration of 100 μM, DISO nearly abolished I_{hERG} (Fig. 3Ai); in contrast the current was only little altered by **1**. Fig. 3B shows mean concentration–response plots for 3 concentrations of each of DISO and **1**. The derived IC_{50} for DISO inhibition of I_{hERG} was 7.56 ± 0.54 μM, close to previously reported values [13,26] and within therapeutic plasma levels of 6–8 μM [27]. By contrast, at concentrations between 10 μM and 1 mM, **1** produced comparatively little I_{hERG} block; even at 1 mM the compound produced less than 30% mean I_{hERG} inhibition. Higher concentrations could not be tested, and as no tested concentration produced > 50% inhibition an accurate experimentally derived IC_{50} could not be obtained, though it is likely to approximate or exceed 10 mM.

Our I_{hERG} data indicate that at micromolar concentrations **1** produces little I_{hERG} inhibition, unlike the parent compound. Mutagenesis and in silico docking data have located the DISO binding site on hERG low within the channel's inner cavity; the drug is able to make aromatic stacking interactions with aromatic residues on the S6 helix that line the inner cavity [26], whilst the protonated tertiary amino group can make cation-π interactions [26]. 2-Aryl-2-(piridin-2-yl)acetamides lack an alkylamino chain and this appears radically to reduce the inhibition of hERG; presumably the smaller molecule is less well able to make contacts to key binding residues, as has been observed previously for structurally similar Ranolazine and (smaller) Lidocaine [28].

The dialkylaminoethyl moiety attached to biarylmethyl system present in DISO resembles common pharmacophore patterns not only for hERG inhibitors, but is also a characteristic structural motif present in several muscarinic cholinergic (M) receptor ligands [29,30]. Moreover, it has been shown that DISO binds this receptor and produces anticholinergic effects in heart tissue [31], which might contribute to its cardiac effects. Therefore, we compared inhibitory activities of DISO and a representative 2-Aryl-2-(piridin-2-yl)acetamide **1** on binding of [^{3}H]-Quinuclidinyl benzilate ([^{3}H]-QNB) to Wistar Rat M receptors, at clinically relevant concentration of 10 μM (Table 11). We found out that, in contrast to DISO, **1** did not inhibit binding of [^{3}H]-QNB to M receptors, which might be another feature determining its increased cardiac safety. Indeed, in addition to its high *in vivo* cardiac safety in

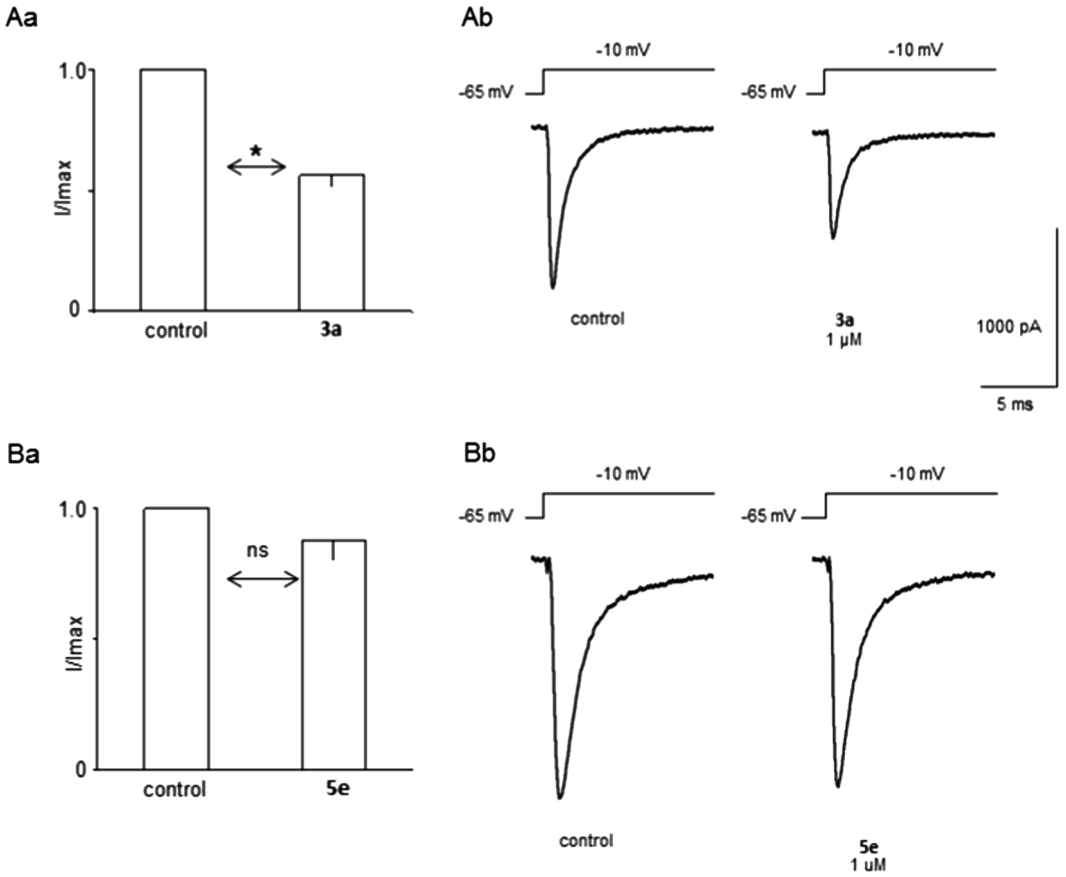

Fig. 2. A: Compound **3a** potently inhibits voltage-gated Na^+ currents in prefrontal cortex pyramidal neurons. Aa: Averaged normalized maximal Na^+ currents amplitudes are shown. Ab: Example recordings of Na^+ currents in control and in the presence of **3a** (1 μM). B: **5e** slightly inhibits voltage-gated Na^+ currents. Ba: Averaged normalized maximal Na^+ currents amplitudes are shown. Bb: Example recordings of Na^+ currents in control and in the presence of **5e** (1 μM).

rats [8], the compound did not trigger cardiotoxicity in guinea pigs or rabbits (see: Supplementary Material).

3. Conclusions

We have synthesized a number of 2-aryl-2-(pyridin-2-yl)acetamide derivatives and subjected them for screening in animal models of epilepsy within the ETPS of NIH. The SAR of the phenyl substituents showed that the *para-* position was clearly disfavored. Analyzing the type of substituents we observed a general trend that –OMe derivatives were inactive. Compounds bearing a larger naphthalene ring were slightly less active to the benzene derivatives, whereas the pyridine bioisoster completely lacked the desired anticonvulsant activity. Modifications of the amide functional group yielded highly active nitriles or secondary amides that were generally less potent in antiseizure models.

Notwithstanding distinctive SAR trends within the series, the investigated arylacetamides display a markedly broader spectrum of activity in animal models of epilepsy than the reference 'classical' sodium channel blocking AEDs. Above all, this enhancement is manifested by higher activities of the compounds in the 'classical' scMET model, as well as in the 6 Hz and kindling models of pharmacoresistant seizures.

The results of the patch-clamp experiments show that the compounds block voltage-gated sodium channel. Intriguingly, besides the **3a–5e** molecular pair, there is no distinct correlation between the potency of inhibition of the normalized maximal amplitudes of neuronal sodium currents and the ED_{50} values of the compounds in the *in vivo* epilepsy models. On one hand, this could be due to the possible variations in their ADME/PK profiles. Nevertheless, additional mechanisms of action cannot be ruled out, which is supported by the broader *in vivo* activity pattern of the compounds than it would have been expected for the sodium current inhibition alone.

The 2-aryl-2-(pyridin-2-yl)acetamides have been derived from DISO, a known hERG potassium channel blocker and M receptor binder. Here, we found that a representative compound from the series, **1**, lacks these undesirable, cardiotoxicity-triggering features, most likely due to the absence of the alkylamino chain of the parent compound. As a result, the compound is characterized by an excellent *in vivo* cardiac safety, which, along with its broad anticonvulsant activity in rodent models and a proper ADME/PK profile (see: Supplementary Material), may merit further investigations on 2-aryl-2-(pyridin-2-yl)acetamide scaffold.

4. Experimental section

4.1. Chemistry

Melting points were determined on an Electrothermal 9100 apparatus in open capillary tubes and were uncorrected. Elemental analyses were performed using Elementar Vario EL III. The NMR spectra were obtained on a Varian Inova 500 MHz, a Bruker AVHD400 or a Bruker AVHD300 spectrometer. Chemical shifts (δ) were expressed in parts per million (ppm) relative to tetramethylsilane (TMS) or solvent used as the internal reference. The following abbreviations were used to describe the peak patterns: s (singlet), d (doublet), t (triplet), q (quartet), qt (quintet), m (multiplet), p (pseudo-) and b (broad-). Coupling constants (*J*) were in hertz (Hz). Thin-layer chromatography (TLC) was run on Merck Silica gel-60 F254 plates. The spots were visualised by ultraviolet light (254 nm) or iodine vapors. Flash column chromatography (FC) was carried out on Merck Silica gel 60 (particle size: 0.040–0.063 mm).

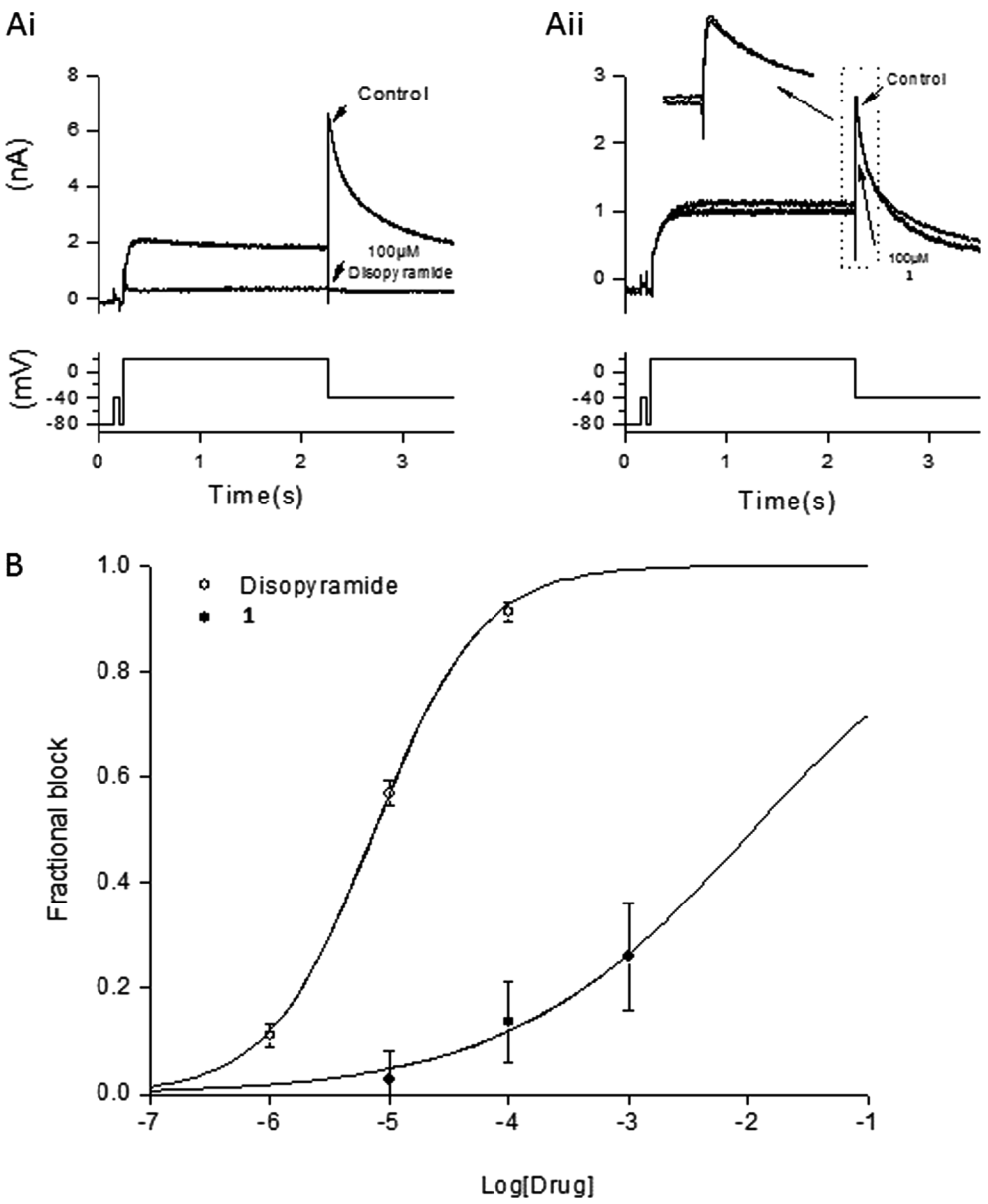

Fig. 3. A: I_{hERG} traces elicited in control conditions and following exposure to 100 μM of DISO (Ai) and **1** (Aii). In each panel the voltage protocol is shown as the lower trace. 100 μM DISO nearly completely abolished I_{hERG} (Ai), but at the same concentration **1** produced little I_{hERG} Inhibition. Inset to Aii shows expanded I_{hERG} tails, underscoring the small degree of inhibition seen with **1**. B: Concentration-response plots for effects of 100 μM DISO and **1** on I_{hERG} tails (n ≥ 6 for each concentration for both compounds). I_{hERG} tail amplitude was measured as difference between peak outward tail current and the current elicited by the brief prepulse to −40 mV that preceded the test depolarisation. Mean ± SEM fractional block is plotted for each concentration of the two compounds. A fit to the DISO data with a standard Hill equation gave an IC_{50} of 7.56 ± 0.54 μM, with a Hill slope (n_H) of 0.98 ± 0.07. The highest concentration of **1** tested was 1 mM, which produced < 30% mean fractional inhibition. Higher concentrations were not possible to obtain due to poor solubility at such concentrations. A complete dose-response fit was not possible, but the IC_{50} is likely to approximate or exceed 10 mM.

Table 11
Inhibition of binding of [^{3}H]-Quinuclidinyl benzilate ([^{3}H]-QNB) to Wistar Rat cerebral cortex muscarinic cholinergic receptors by DISO and ADD424042.

Compound	% inhibition[a]
DISO	52%
1	−14%

[a] 10 μM of a test compound, n = 3.

Solvents were dried and purified by standard methods. All reagents were purchased from commercial sources and used as received. Solvents for chromatography were distilled prior use. The purities of final compounds were ≥95%, (LC/MS and/or elemental analysis), according to ETSP dispositions. Compounds **1**, **2a**, **2d**, **3a**, **3b**, **3c**, **3d**, **3j**, **3k**, **3l**, **3m** were synthesized as described previously [32].

4.1.1. 2-methyl-2-phenyl-2-(pyridin-2-yl)acetonitrile (2r)

To a stirred, cooled (-78 °C) solution of 2-phenyl-2-(pyridin-2-yl) acetonitrile **2a** (4.10 g, 21.1 mmol) in dry THF (75 mL) was added Lithium *N*,*N*-Diisopropylamide (25.4 mL of 1 M solution in THF, 25.4 mmol, 1.2 eq.), dropwise. The solution was stirred for 1 h and Methyl Iodide (1.45 mL, 23.2 mmol, 1.1 eq.) was added dropwise. The mixture was brought to room temperature and stirred overnight. The reaction was quenched with saturated aqueous solution of NH_4Cl (75 mL). The mixture was extracted with AcOEt (2 × 75 mL). The organic extracts were washed with saturated aqueous solution of NaCl (2 × 50 mL), dried over anhydrous Na_2SO_4, filtered and concentrated. The residue was purified by FC (hexane/AcOEt 6:1 to 2:1). Colorless oil (3.67 g, 76%); ^{1}H NMR (400 MHz, $CDCl_3$): δ = 8.65 (ddd, J = 5.0, 2.0, 1.0, 1H), 7.71 (td, J = 8.0, 2.0, 1H), 7.51–7.44 (m, 3H), 7.42–7.36 (m, 2H), 7.35–7.30 (m, 1H), 7.26 (ddd, J = 7.5, 5.0, 1.0, 1H), 2.21 (s, 3H); ^{13}C NMR (101 MHz, $CDCl_3$): δ = 159.1, 149.3, 140.4, 137.3, 129.0, 128.0, 126.4, 123.0, 122.9, 121.8, 48.7, 26.9; MS (ESI+): *m/z* 209 [M + H]$^+$

4.1.2. 2-fluoro-2-phenyl-2-(pyridin-2-yl)acetonitrile (2 s)

To a stirred, cooled (-78 °C) solution of 2-phenyl-2-(pyridin-2-yl) acetonitrile **2a** (2.80 g, 14.4 mmol) in dry THF (50 mL) was added Lithium *N*,*N*-Diisopropylamide (17.3 mL of 1 M solution in THF, 17.3 mmol, 1.2 eq.), dropwise. The resulting solution was stirred for 1 h

and *N*-Fluorodi(benzenesulfonyl)amine (5.00 g, 15.9 mmol, 1.1 eq.) was added portionwise, over 10 min. The mixture was brought to room temperature and stirred overnight. The reaction was quenched with saturated aqueous solution of NH_4Cl (50 mL). The mixture was extracted with AcOEt (2 × 50 mL). The organic extracts were washed with saturated aqueous solution of NaCl (2 × 25 mL), dried over anhydrous Na_2SO_4, filtered and concentrated. The residue was purified by FC (hexane/AcOEt 8:1 to 5:1). Pale-yellow oil (2.15 g, 70%); ^{1}H NMR (300 MHz, $CDCl_3$): δ = 8.70 (ddt, J = 5.0, 2.0, 1.0, 1H), 7.85 (td, J = 8.0, 2.0, 1H), 7.63 (dq, J = 8.0, 1.0, 1H), 7.61–7.56 (m, 2H), 7.53–7.42 (m, 3H), 7.38 (ddd, J = 7.5, 5.0, 1.5, 1H); ^{13}C NMR (75 MHz, $CDCl_3$): δ = 155.2 (d, J = 28.5), 149.8 (d, J = 2.0), 137.7, 135.9 (d, J = 24.0), 130.3 (d, J = 2.0), 129.0, 125.87 (d, J = 5.5), 124.6 (d, J = 1.5), 119.7 (d, J = 5.5), 116.7 (d, J = 33.5), 92.1 (d, J = 185.5); MS (ESI+): m/z 234 $[M+Na]^+$

4.1.3. General procedure for synthesis of 3e–i and 3n–q

Appropriate starting arylacetonitrile (1 eq.) was added to a stirred suspension of KOH (5 eq.) in DMSO (200 mL per 1 mol of KOH). The mixture was brought to 60 °C. Bromopyridine (1.5 eq.) was then added dropwise, at 60–70 °C, followed by further stirring at this temperature for 4 h. The reaction mixture was cooled and poured onto water (500 mL) and the resulting cloudy solution was extracted with AcOEt (2 × 150 mL), washed with water (100 mL) and brine (100 mL). The organic extract was dried over anhydrous $MgSO_4$, filtered and concentrated under reduced pressure. The residue was dissolved in AcOH (100 mL) and concentrated H_2SO_4 (35 mL). The solution was heated at 100 °C until TLC showed complete reaction (1–3 h). The solution was cooled and poured onto excess of ice-25% aqueous ammonia. The resulting mixture was extracted with CH_2Cl_2 (3 × 75 mL). The combined organic extracts were washed with water (2 × 75 mL), brine (75 mL), dried over anhydrous Na_2SO_4, filtered and evaporated. The title compounds were purified by recrystallization or by FC.

4.1.4. 2-(3-chlorophenyl)-2-(pyridin-2-yl)acetamide (3e)

3-chlorophenylacetonitrile (15.00 g, 98.9 mmol), 2-bromopyridine (14.16 mL, 160.42 mmol) and KOH (25.52 g, 494.5 mmol), recrystallization from *n*-hexane/AcOEt 1:1 (v/v). White powder (9.81 g, 37%); mp: 96–97 °C; ^{1}H NMR (500 MHz, $CDCl_3$): δ = 8.60 (d, J = 4.5, 1H), 7.85 (bs, 1H), 7.67 (td, J = 7.5, 1.5, 1H), 7.43 (s, 1H), 7.32–7.34 (m, 1H), 7.29 (d, J = 8.0, 1H), 7.26–7.20 (m, 3H), 6.12 (bs, 1H), 4.98 (s, 1H); ^{13}C NMR (125 MHz, $CDCl_3$): δ = 172.6, 157.9, 149.1, 140.5, 137.5, 134.5, 129.9, 128.4, 127.6, 126.6, 124.4, 122.5, 59.9; MS (ESI+): m/z 269 $[M+Na]^+$; Anal. calcd for $C_{13}H_{11}ClN_2O$: C 63.29, H 4.49, N 11.36, found: C 63.40, H 4.55, N 11.28.

4.1.5. 2-(3-methylphenyl)-2-(pyridin-2-yl)acetamide (3f)

3-methylphenylacetonitrile (15.00 g, 114.3 mmol), 2-bromopyridine (15.13 mL, 171.5 mmol) and KOH (32.06 g, 571.5 mmol), recrystallization from *n*-hexane/AcOEt 1:1 (v/v). White powder (15.02 g, 53%); mp: 96–97 °C; ^{1}H NMR (500 MHz, $CDCl_3$): δ = 8.59 (d, J = 4.0, 1H), 7.67 (bs, 1H), 7.64 (td, J = 7.5, 2.0, 1H), 7.28 (d, J = 8.0, 1H), 7.23 (s, 1H), 7.22–7.16 (m, 3H), 7.06 (d, J = 6.5, 1H), 6.00 (bs, 1H), 4.98 (s, 1H), 2.31 (s, 3H); ^{13}C NMR (125 MHz, $CDCl_3$): δ = 173.4, 158.8, 149.0, 138.6, 138.4, 137.2, 129.0, 128.6, 128.2, 125.3, 124.4, 122.2, 60.5, 21.4; MS (ESI+): m/z 249 $[M+Na]^+$; Anal. calcd for $C_{14}H_{14}N_2O$: C 74.31, H 6.24, N 12.38, found: C 74.25, H 6.37, N 12.30.

4.1.6. 2-(3-methoxyphenyl)-2-(pyridin-2-yl)acetamide (3g)

3-methoxylphenylacetonitrile (12.00 g, 81.5 mmol), 2-bromopyridine (10.79 mL, 122.3 mmol) and KOH (22.86 g, 407.5 mmol), recrystallization from *n*-hexane/AcOEt 1:1 (v/v). White powder (8.82 g, 41%); mp: 62–64 °C; ^{1}H NMR (500 MHz, $CDCl_3$): δ = 8.59 (d, J = 4.0, 1H), 7.69 (bs, 1H), 7.64 (td, J = 8.0, 2.0, 1H), 7.29 (d, J = 8.0, 1H), 7.25–7.17 (m, 2H), 7.02–6.97 (m, 2H), 6.79 (dt, J = 8.0, 2.0, 1H), 5.84 (bs, 1H), 4.98 (s, 1H), 3.76 (s, 3H); ^{13}C NMR (125 MHz, $CDCl_3$): δ = 173.1, 159.8, 158.5, 149.0, 140.1, 137.3, 129.7, 124.4, 122.3, 120.7, 114.2, 112.8, 60.5, 55.2; MS (ESI+): m/z 265 $[M+Na]^+$; Anal. calcd for $C_{11}H_{14}N_2O_2$: C 69.41, H 5.82, N 11.56, found: C 69.49, H 5.99, N 11.52.

4.1.7. 2-(3-fluorophenyl)-2-(pyridin-2-yl)acetamide (3h)

3-fluorophenylacetonitrile (10.00 g, 74.0 mmol), 2-bromopyridine (9.79 mL, 111.0 mmol) and KOH (20.78 g, 370.0 mmol), recrystallization from *n*-hexane/AcOEt 1:1 (v/v). White powder (6.53 g, 35%); mp: 95–96 °C; ^{1}H NMR (500 MHz, $CDCl_3$): δ = 8.60 (d, J = 4.0, 1H), 7.82 (bs, 1H), 7.67 (td, J = 7.5, 2.0, 1H), 7.32–7.14 (m, 5H), 6.94 (dt, J = 8.5, 1.5, 1H), 6.18 (bs, 1H), 5.01 (s, 1H); ^{13}C NMR (125 MHz, $CDCl_3$): δ = 172.7, 162.8 (d, J = 246.3), 158.0, 141.0 (d, J = 7.5), 137.4, 130.1 (d, J = 8.5), 124.4, 124.1 (d, J = 3.0), 122.5, 115.3 (d, J = 22.5), 114.3 (d, J = 21.0), 60.0; MS (ESI+): m/z 253 $[M+Na]^+$; Anal. calcd for $C_{13}H_{11}FN_2O$: C 67.82, H 4.82, N 12.17, found: C 67.90, H 5.01, N 11.98.

4.1.8. 2-(3-trifluoromethylphenyl)-2-(pyridin-2-yl)acetamide (3i)

3-trifluorophenylacetonitrile (10.00 g, 54.0 mmol), 2-bromopyridine (9.79 mL, 81.0 mmol) and KOH (15.15 g, 270.0 mmol), recrystallization from *n*-hexane/AcOEt 1:1 (v/v). White powder (7.26 g, 48%); mp: 116–118 °C; ^{1}H NMR (500 MHz, $CDCl_3$): δ = 8.62 (d, J = 4.0, 1H), 7.91 (bs, 1H), 7.74–7.62 (m, 3H), 7.51 (d, J = 8.0, 1H), 7.42 (t, J = 8.0, 1H), 7.30 (d, J = 8.0, 1H), 7.27–7.21 (m, 1H), 6.12 (bs, 1H), 5.05 (s, 1H); ^{13}C NMR (125 MHz, $CDCl_3$): δ = 172.5, 157.8, 149.2, 139.6, 137.6, 131.8, 131.0 (q, J = 32.0), 129.1, 125.1 (q, J = 3.0), 124.4, 124.3 (q, J = 4.0), 124.0 (q, J = 272.5), 122.7, 60.0; MS (ESI+): m/z 281 $[M+H]^+$; Anal. calcd for $C_{14}H_{11}F_3N_2O$: C 60.00, H 3.96, N 9.99, found: C 59.72, H 4.12, N 9.97.

4.1.9. 2-(3,4-dichlorophenyl)-2-(pyridin-2-yl)acetamide (3n)

From 3,4-dichlorophenylacetonitrile (10.00 g, 53.8 mmol), 2-bromopyridine (7.70 mL, 80.6 mmol) and KOH (15.00 g, 269.0 mmol), recrystallization from DCM. White powder (7.07 g, 47%); mp: 146–147 °C; ^{1}H NMR (500 MHz, $CDCl_3$): δ = 8.62 (d, J = 4.5, 1H), 7.90 (bs, 1H), 7.70 (td, J = 7.5, 1.5, 1H), 7.55 (d, J = 2.0, 1H), 7.38 (d, J = 8.5, 1H), 7.33–7.23 (m, 3H), 5.82 (bs, 1H), 4.93 (s, 1H); ^{13}C NMR (125 MHz, $CDCl_3$): δ = 172.3, 157.8, 149.5, 139.0, 137.9, 133.0, 131.9, 130.8, 130.5, 128.0, 124.7, 123.0, 59.6; Anal. calcd for $C_{14}H_{14}N_2O$: C 55.54, H 3.59, N 9.96, found: C 55.49, H 3.64, N 10.12.

4.1.10. 2,2-di(pyridin-2-yl)acetamide (3o)

From 2-pyridylacetonitrile (25.00 g, 211.6 mmol), 2-bromopyridine (30.32 mL, 317.4 mmol) and KOH (59.35 g, 1058.0 mmol), recrystallization from *n*-hexanes/AcOEt 2:3 (v/v). White powder (10.79 g, 24%); mp: 186–187 °C; ^{1}H NMR (500 MHz, $CDCl_3$): δ = 8.58 (ddd, J = 5.0, 2.0, 1.0, 2H), 8.23 (bs, 1H), 7.67 (td, J = 7.5, 1.5, 2H), 7.44 (d, J = 7.5, 2H), 7.19 (ddd, J = 6.0, 5.0, 1.0, 2H), 5.95 (bs, 1H), 5.25 (s, 1H); ^{13}C NMR (125 MHz, $CDCl_3$): δ = 172.0, 157.9, 149.3, 137.2, 123.8, 122.4, 62.8; MS (ESI+): m/z 214 $[M+H]^+$; Anal. calcd for $C_{12}H_{11}N_3O$: C 67.58, H 5.21, N 19.71, found: C 67.56, H 5.20, N 19.61.

4.1.11. 2-(1-naphthyl)-2-(pyridin-2-yl)acetamide (3p)

From 1-naphthylacetonitrile (19.00 g, 113.6 mmol), 2-bromopyridine (16.28 mL, 170.4 mmol) and KOH (31.67 g, 568.0 mmol), recrystallization from *n*-hexanes/AcOEt 2:3 (v/v). White powder (6.02 g, 20%); mp: 103–106 °C; ^{1}H NMR (500 MHz, $CDCl_3$): δ = 8.61 (ddd, J = 5.0, 2.0, 1.0, 1H), 8.14 (pd, J = 8.0, 1H), 7.86 (dd, J = 7.5, 2.0, 1H), 7.80 (d, J = 8.5, 1H), 7.64 (td , J = 7.5, 2.0, 1H), 7.58 (d, J = 6.5, 1H), 7.53–7.46 (m, 2H), 7.44 (dd, J = 8.5, 7.0, 1H), 7.26 dt, J = 8.0, 1.0), 7.22 (ddd, J = 7.5, 5.0, 1.5, 1H), 6.92 (bs, 1H), 5.96 (s, 1H), 5.94 (bs, 1H); ^{13}C NMR (125 MHz, $CDCl_3$): δ = 173.1, 158.4, 148.2, 137.8, 134.1, 131.7, 128.9, 128.6, 126.8, 126.3, 125.9, 125.5, 124.8, 123.6, 122.5, 56.3; MS (ESI+): m/z 263 $[M+H]^+$; Anal. calcd for $C_{17}H_{14}N_2O$:

C 77.54, H 5.38, N 10.68, found: C 77.32, H 5.39, N 10.40.

4.1.12. 2-(2-naphthyl)-2-(pyridin-2-yl)acetamide (3q)

From 1-naphthylacetonitrile (10.00 g, 59.8 mmol), 2-bromopyridine (8.57 mL, 89,68 mmol) and KOH (16.77 g, 299.0 mmol), FC (CH_2Cl_2/MeOH 99:1 to 95:5, v/v). White powder (4.20 g, 27%); mp: 136–137 °C; ^{1}H NMR (500 MHz, $CDCl_3$): δ = 8.61 (ddd, J = 5.0, 1.5, 1.0, 1H), 8.86 (d, J = 1.0, 1H), 7.80–7.75 (m, 3H), 7.73 (bs, 1H), 7.66 (td, J = 8.0, 2.0, 1H), 7.55 (dd, J = 8.5, 2.0, 1H), 7.46–7.41 (m, 2H), 7.34 (dt, J = 8.0, 1.0, 1H), 7.21 (ddd, J = 8.0, 5.0, 1.0, 1H), 6.06 (bs, 1H), 5.24 (s, 1H); ^{13}C NMR (125 MHz, $CDCl_3$): δ = 173.1, 158.5, 148.7, 137.5, 136.0, 133.4, 132.6, 128.5, 128.0, 127.5, 127.2, 126.3, 126.2, 126.1, 124.6, 122.4, 60.3; MS (ESI+): m/z 263 $[M+H]^+$; Anal. calcd for $C_{17}H_{14}N_2O$: C 77.54, H 5.38, N 10.68, found: C 77.71, H 5.44, N 10.68.

General procedure for synthesis of 3r,s. **2r** or **2s** was dissolved in AcOH (50 mL) and concentrated H_2SO_4 (18 mL). The solution was heated at 100 °C until TLC showed complete reaction (1–3 h). The solution was cooled and poured onto excess of ice-25% aqueous ammonia. The resulting mixture was extracted with CH_2Cl_2 (3 × 35 mL). The combined organic extracts were washed with water (2 × 35 mL), brine (35 mL), dried over anhydrous Na_2SO_4, filtered and evaporated. The title compounds were purified by FC.

4.1.13. 2-methyl-2-phenyl-2-(pyridin-2-yl)acetamide (3r)

From **2r** (3.10 g, 14.9 mmol), FC (CH_2Cl_2/MeOH 99:1 to 95:5, v/v). White powder (2.37 g, 70%); mp: 141–143 °C; ^{1}H NMR (300 MHz, $CDCl_3$): δ = 8.63 (ddd, J = 5.0, 2.0, 1.0, 1H), 7.81–7.69 (m, 1H), 7.54–7.37 (m, 2H), 7.38–7.22 (m, 4H), 7.20–7.14 (m, 2H), 6.00 (bs, 1H), 2.01 (s, 3H); ^{13}C NMR (75 MHz, $CDCl_3$): δ = 176.4, 163.1, 148.4, 145.7, 137.3, 128.5, 127.6, 126.9, 122.8, 122.1, 58.4, 26.2; MS (ESI+): m/z 227 $[M+H]^+$; Anal. calcd for $C_{14}H_{14}N_2O$: C 74.31, H 6.24, N 12.38, found: C 74.47, H 6.26, N 12.32.

4.1.14. 2-fluoro-2-phenyl-2-(pyridin-2-yl)acetamide (3s)

From **2 s** (1.90 g, 8.95 mmol), FC (CH_2Cl_2/MeOH 99:1 to 97:3, v/v). White powder (1.52 g, 74%); mp: 168–169 °C; ^{1}H NMR (400 MHz, $CDCl_3$): δ = 8.62–8.59 (m, 1H), 7.66 (td, J = 8.0, 2.0, 1H), 7.51 (m, 2H), 7.41 (dt, J = 8.0, 1.0, 1H), 7.33–7.29 (m, 3H), 7.26–7.21 (m, 1H), 7.17 (bs, 1H), 6.28 (bs, 1H); ^{13}C NMR (101 MHz, $CDCl_3$): δ = 171.0 (d, J = 25.0), 157.3 (d, J = 24.0 Hz), 148.9, 137.4 (d, J = 22.0), 137.2, 129.2 (d, J = 2.0), 128.4, 126.6 (d, J = 7.5), 123.8 (d, J = 2.0 Hz), 122.3 (d, J = 6.5 Hz), 97.8 (d, J = 188.5 Hz); MS (ESI+): m/z 231 $[M+H]^+$; Anal. calcd for $C_{13}H_{11}N_2FO$: C 67.82, H 4.82, N 12.17, found: C 67.61, H 4.79, N 12.04.

4.1.15. Methyl 2-phenyl-2-(piridin-2yl)acetate (4)

2-phenyl-2-(pyridin-2-yl)acetonitrile **2a** (5.40 g, 27.8 mmol) was dissolved in saturated methanolic solution of HCl (60 mL), at 4 °C. The mixture was left overnight at room temperature. The resulting clear solution was diluted with water (150 mL) and brought to pH 10 with 3 N aqueous solution of NaOH. The resulting mixture was extracted with AcOEt (3 × 100 mL). The combined organic extracts were washed with brine (100 mL), dried over anhydrous MgSO4, filtered and concentrated under reduced pressure. The crude product was recrystallized from EtOH. White powder (3.90 g, 62%); mp: 74–76 °C; ^{1}H NMR (500 MHz, $CDCl_3$): δ = 3.76 (s, 3H), 5.24 (s, 1H), 7.16 (ddd, J = 7.5, J = 5.0, J = 1.0, 1H), 7.22 (dt, J = 8.0, J = 1.0, 1H), 7.28 (tt, J = 7.0, J = 1.5, 1H), 7.32–7.37 (m, 2H), 7.37–7.41 (m, 2H), 7.60 (td, J = 7.5, J = 2.0, 1H), 8.57 (ddd, J = 5.0, J = 2.0, J = 1.0, 1H); ^{13}C NMR (125 MHz, $CDCl_3$): δ = 52.4, 59.6, 122.1, 123.0, 127.6, 128.7 20.4, 60.5, 122.1, 124.4, 127.2, 128.2, 128.6, 128.9, 136.7, 137.1, 149.3, 158.6, 172.2; MS (ESI+): m/z 228 $[M+H]^+$; Anal. calcd for $C_{14}H_{13}N_1O_2$: C 73.98, H 5.78, N 6.16, found: C 74.09, H 5.75, N 6.33.

4.1.16. General procedure for synthesis of 5a–e

A mixture of methyl 2-phenyl-2-(piridin-2yl)acetate **3** (1.0 eq.), amine (10.0 eq.), TBD (0.3 eq.) in THF (2 mL per 1 mmol of **3**) was refluxed for 3 h. The resulting solution was cooled, concentrated under reduced pressure and purified by FC (CH_2Cl_2/MeOH 99:1 to 95:5, v/v).

4.1.17. N-methyl-2-phenyl-2-(piridin-2yl)acetamide (5a)

White powder (1.85 g, 93%); mp: 129–130 °C; ^{1}H NMR (500 MHz, $CDCl_3$): δ = 2.83 (d, J = 4.5 Hz, 3H), 5.02 (s, 1H), 7.19 (ddd, J = 7.5, J = 5.0, J = 1.0, 1H), 7.26 (tt, J = 6.0, J = 1.0, 1H), 7.23–7.31 (m, 3H), 7.36–7.40 (m, 2H), 7.64 (td, J = 7.5, J = 2.0, 1H), 7.78 (bs, 1H), 8.58 (ddd, J = 5.0, J = 2.0, J = 1.0, 1H); ^{13}C NMR (125 MHz, $CDCl_3$): δ = 20.4, 60.5, 122.1, 124.4, 127.2, 128.2, 128.6, 137.2, 139.0, 148.8, 158.9, 171.2; MS (ESI+): m/z 227 $[M+H]^+$; Anal. calcd for $C_{14}H_{14}N_2O$: C 74.31, H 6.24, N 12.38, found: C 74.04, H 6.24, N 12.24.

4.1.18. N-ethyl-2-phenyl-2-(piridin-2yl)acetamide (5b)

White powder (2.01 g, 94%); mp: 120–122 °C; ^{1}H NMR (500 MHz, $CDCl_3$): δ = 1.01 (t, J = 7.0, 3H), 3.12 (dq, J = 7.0 Hz, J = 1.5, 2H), 5.10 (s, 1H), 7.21–7.26 (m, 2H), 7.29–7.33 (m, 2H), 7.35–7.39 (m, 2H), 7.71 (td, J = 7.5, J = 2.0, 1H), 8.35 (bt, J = 5.5), 8.49 (ddd, J = 7.5, J = 2.0, 1H); ^{13}C NMR (125 MHz, $CDCl_3$): δ = 14.6, 33.7 50.5, 121.9, 122.9, 126.7, 128.3, 128.6, 136.5, 139.3, 148.7, 159.6, 169.8; MS (ESI+): m/z 241 $[M+H]^+$; Anal. calcd for $C_{15}H_{16}N_2O$: C 74.97, H 6.71, N 11.66, found: C 74.84, H 6.88, N 11.91.

4.1.19. N-propyl-2-phenyl-2-(piridin-2yl)acetamide (5c)

White powder (1.03 g, 92%); mp: 79–80 °C; ^{1}H NMR (500 MHz, $(CD_3)_2CO$): δ = 0.85 (t, J = 7.5, 3H), 1.84 (sx, J = 7.5, 2H), 3.18 (t, J = 7.0, 1H), 3.19 (t, J = 7.0, 1H), 5.10 (s, 1H), 7.20–7.25 (m, 2H), 7.27–7.32 (m, 2H), 7.43–7.48 (m, 3H), 7.71 (td, J = 7.5, J = 2.0, 1H), 7.91 (bs, 1H), 8.52 (ddd, J = 5.0, J = 2.0, J = 1.0, 1H); ^{13}C NMR (125 MHz, $(CD_3)_2CO$): δ = 11.7, 23.5, 41.7, 61.5, 122.8, 124.4, 127.6, 129.1, 129.4, 137.4, 140.7, 149.6, 160.8, 170.9; MS (ESI+): m/z 255 $[M+H]^+$; Anal. calcd for $C_{16}H_{18}N_2O$: C 75.56, H 7.13, N 11.01, found: C 75.78, H 7.02, N 10.76.

4.1.20. N-isopropyl-2-phenyl-2-(piridin-2yl)acetamide (5d)

White powder (1.01 g, 90%); mp: 111–114 °C; ^{1}H NMR (500 MHz, $CDCl_3$): δ = 1.01 (dd, J = 6.5, 6H), 4.09 (m, 1H), 4.96 (s, 1H), 7.19 (ddd, J = 8.0, J = 5.0, J = 1.0, 1H), 7.27–7.32 (m, 3H), 7.23 (tt, J = 7.5, J = 2.0, 1H), 7.36–7.40 (m, 2H), 7.51 (bd, 1H), 7.65 (td, J = 7.5, J = 2.0, 1H), 8.49 (ddd, J = 5.0, J = 2.0, J = 1.0, 1H); ^{13}C NMR (125 MHz, $CDCl_3$): δ = 22.5, 22.6, 41.5, 60.7, 122.1, 124.4, 127.2, 128.1, 128.6, 137.2, 139.2, 148.8, 159.1, 169.6; MS (ESI+): m/z 255 $[M+H]^+$; Anal. calcd for $C_{16}H_{18}N_2O$: C 75.56, H 7.13, N 11.01, found: C 75.43, H 7.05, N 10.56.

4.1.21. N-benzyl-2-phenyl-2-(piridin-2yl)acetamide (4e)

White powder (1.22 g, 91%); mp: 112–115 °C; ^{1}H NMR (500 MHz, $CDCl_3$): δ = 4.48 (dd, J = 15.0, J = 6.0, 1H), 4.52 (dd, J = 15.0, J = 6.0, 1H), 5.07 (s, 1H), 7.18–7.32 (m, 9H), 7.39–7.42 (m, 2H), 7.65 (td, J = 8.0, J = 2.0, 1H), 8.24 (bt, J = 6.0, 1H), 8.55 (ddd, J = 5.0, J = 2.0, J = 1.0, 1H); ^{13}C NMR (125 MHz, $CDCl_3$): δ = 43.5, 60.5, 122.2, 124.5, 127.2, 127.3, 127.4, 128.2, 128.5, 128.7, 137.2, 138.3, 139.0, 148.8, 158.8, 170.6; MS (ESI+): m/z 303 $[M+H]^+$; Anal. calcd for $C_{20}H_{18}N_2O$: 79.44, H 6.00, N 9.26, found: C 79.54, H 5.95, N 8.91.

4.2. Anticonvulsant testing

The compounds were evaluated in the *in vivo* rodent models of epilepsy within the ETSP, according to the well-established experimental procedures and decision schemes described in the PANAChE database [1,6].

4.3. Sodium current recordings

The experimental procedures used in this study adhered to the institutional and international guidelines on the ethical use of animals. The methodology of current recordings was the same as in our previous studies [8]. Briefly, 3-week-old rats were decapitated under ethyl-chloride anaesthesia and their brains were removed. Parts of the slices containing the prefrontal cortex were mechanically and enzymatically dispersed. Pipette solution and extracellular solutions were the same as in our previous study [8]. Currents were recorded using an Axopatch 1D amplifier and analysed with pClamp software (Axon Instruments and Molecular Devices, CA, USA). Patch-pipettes had resistances between 4 and 5 MΩ. The access resistance was between 5 and 7 MΩ. A series resistance compensation of 80% was applied. The sodium currents were leak subtracted. Recordings were performed at room temperature. Voltage-gated potassium currents were not recorded because they were blocked by TEA-CL in the extracellular solution. Voltage-gated calcium currents were blocked by cadmium and lanthanum ions in the extracellular solution. Compounds were applied to the whole-bath.

4.4. hERG electrophysiology

Disopyramide phosphate powder (Sigma, St. Louis, USA) was dissolved in deionised water to give a stock solution of 100 mM, **1** was dissolved in DMSO to make a stock solution of 500 mM, which were then serially diluted to produce stock solutions ranging down to 1 mM. The stock solutions were then diluted 1:1000 fold (except 1 mM **1** which was 2:1000 fold) with Tyrode solution to achieve concentration stated in the 'results' section. For whole-cell patch-clamp recording, HEK 293 cells stably expressing wild-type hERG1a [33] were continuously superfused at 37 °C with an external solution containing (in mM): 140 NaCl, 4 KCl, 2.5 $CaCl_2$, 1 $MgCl_2$, 10 Glucose and 5 HEPES (titrated to pH 7.45 with NaOH). Patch-pipettes (Corning 7052 glass, AM Systems, Sequim, USA) were pulled and heat-polished to 2.5–4 MΩ. The patch pipette solution contained (in mM): 130 KCl, 1 $MgCl_2$, 5 EGTA, 5 MgATP, 10 HEPES (titrated to pH 7.2 using KOH). Recordings were made using an Axopatch 200A amplifier and a CV201 head-stage (Molecular Devices, CA, USA). 70–80% of pipette series resistance was compensated. Voltage commands were generated and currents recorded using pClamp 10 (Molecular Devices, CA, USA) and WinWCP (John Dempster, Strathclyde University, UK).

4.5. Radiologand binding assays

Inhibition of [^{3}H]-Quinuclidinyl benzilate ([^{3}H]-QNB) to Wistar Rat cerebral cortex muscarinic cholinergic receptors studies by DISO and **1** were performed commercially by Cerep Laboratories (Poitiers, France), according to the in-house established testing procedures.

Declaration of Competing Interest

The authors declare that they have no known competing financial interests or personal relationships that could have appeared to influence the work reported in this paper.

Acknowledgements

The authors would like to thank the Epilepsy Therapy Screening Program (formerly: Anticonvulsant Screening Program) of National Institute of Neurological Disorders and Stroke (NIND), Rockville, USA staff for providing the results of anticonvulsant testing. Financial support was provided by the Polish Ministry of Science and Higher Education (MD, MK, Grant 'Iuventus Plus' no. IP2012-008372); the Ministry of Education, Youth and Sports of the Czech Republic (the National Sustainability Program I, Project LO1503) and by the Charles University (program for the Development of Scientific Fields, Progress Q39). YZ, AEH and JCH acknowledge support from the British Heart Foundation (PG/12/69/29784; PG/14/61/31015) and Heart Research UK (RG2640).

Appendix A. Supplementary material

Supplementary data to this article can be found online at https://doi.org/10.1016/j.bioorg.2020.103717.

References

[1] S. Abramovici, A. Bagic, Epidemiology of epilepsy, Handbook Clin. Neurol. 138 (2016) 159–171.
[2] E. Perucca, J. French, M. Bialer, Development of new antiepileptic drugs: challenges, incentives, and recent advances, Lancet Neurol. 6 (9) (2007) 793–804.
[3] A.C. Gerlach, J.L. Krajewski, Antiepileptic drug discovery and development: what have we learned and where are we going? Pharmaceuticals (Basel, Switzerland) 3 (9) (2010) 2884–2899.
[4] K.K. Borowicz, M. Banach, Antiarrhythmic drugs and epilepsy, Pharmacol. Rep. 66 (4) (2014) 545–551.
[5] P.L. van der Peet, S. Sandanayake, B. Jarrott, S.J. Williams, Discovery of N-aryloxypropylbenzylamines as voltage-gated sodium channel NaV1.2-subtype-selective inhibitors, ChemMedChem 14 (5) (2019) 570–582.
[6] Public Access to Neuroactive & Anticonvulsant Chemical Evaluations (PANAChE) Database. https://panache.ninds.nih.gov/.
[7] J.H. Kehne, B.D. Klein, S. Raeissi, S. Sharma, The National Institute of Neurological Disorders and Stroke (NINDS) Epilepsy Therapy Screening Program (ETSP), Neurochem. Res. 42 (7) (2017) 1894–1903.
[8] M. Krol, M. Ufnal, B. Szulczyk, P. Podsadni, A. Drapala, J. Turlo, M. Dawidowski, Characterization of Disopyramide derivative ADD424042 as a non-cardiotoxic neuronal sodium channel blocker with broad-spectrum anticonvulsant activity in rodent seizure models, Eur. J. Pharm. Sci. : Off. J. Eur. Federat. Pharm. Sci. 81 (2016) 42–51.
[9] H.S. Sidhu, A. Sadhotra, Current status of the new antiepileptic drugs in chronic pain, Front. Pharmacol. 7 (2016) 276.
[10] M. Bialer, Why are antiepileptic drugs used for nonepileptic conditions? Epilepsia 53 (Suppl 7) (2012) 26–33.
[11] A. Bhattacharya, A.D. Wickenden, S.R. Chaplan, Sodium channel blockers for the treatment of neuropathic pain, Neurother. : J. Am. Soc. Experimental NeuroTherapeutics 6 (4) (2009) 663–678.
[12] A. Tjolsen, O.G. Berge, S. Hunskaar, J.H. Rosland, K. Hole, The formalin test: an evaluation of the method, Pain 51 (1) (1992) 5–17.
[13] A.A. Paul, H.J. Witchel, J.C. Hancox, Inhibition of HERG potassium channel current by the class 1a antiarrhythmic agent disopyramide, Biochem. Biophys. Res. Commun. 280 (5) (2001) 1243–1250.
[14] T. Nakajima, Y. Kurachi, H. Ito, R. Takikawa, T. Sugimoto, Anti-cholinergic effects of quinidine, disopyramide, and procainamide in isolated atrial myocytes: mediation by different molecular mechanisms, Circulat. Res. 64 (2) (1989) 297–303.
[15] K. Romero, R.L. Woosley, Chapter 18 - clinical pharmacology of antiarrhythmic drugs, in: E.M. Antman, M.S. Sabatine (Eds.), Cardiovascular Therapeutics: A Companion to Braunwald's Heart Disease (Fourth Edition), W.B. Saunders, Philadelphia, 2013, pp. 343–364.
[16] F. Herold, A. Chodkowski, Ł. Izbicki, J. Turło, M. Dawidowski, J. Kleps, G. Nowak, K. Stachowicz, M. Dybała, A. Siwek, A.P. Mazurek, A. Mazurek, F. Plucíński, Novel 4-aryl-pyrido[1,2-c]pyrimidines with dual SSRI and 5-HT1A activity. Part 3. Eur. J. Med. Chem. 2011, 46 (1), 142–149.
[17] F. Herold, E. Helbin, M. Król, I. Wolska, J. Kleps, Synthesis and structure of novel 4-arylhexahydro-1H,3H-pyrido[1,2-c]pyrimidine derivatives, J. Heterocyclic Chem. 36 (2) (1999) 389–396.
[18] C. Sabot, K.A. Kumar, S. Meunier, C. Mioskowski, A convenient aminolysis of esters catalyzed by 1,5,7-triazabicyclo[4.4.0]dec-5-ene (TBD) under solvent-free conditions, Tetrahedron Lett. 48 (22) (2007) 3863–3866.
[19] M.E. Barton, B.D. Klein, H.H. Wolf, H. Steve White, Pharmacological characterization of the 6 Hz psychomotor seizure model of partial epilepsy, Epilepsy Res. 47 (3) (2001) 217–227.
[20] H. Klitgaard, Levetiracetam: the preclinical profile of a new class of antiepileptic drugs? Epilepsia 42 (Suppl 4) (2001) 13–18.
[21] A.K.W. Srivastava, H. Steve, Felbamate is effective against behavioral and the electrographic seizures in the Lamotrigine-resistant amygdala kindled rat model of refractory epilepsy, Epilepsia 47 (S4) (2006) 321–322.
[22] A.K. Srivastava, H.S. White, Carbamazepine, but not valproate, displays pharmacoresistance in lamotrigine-resistant amygdala kindled rats, Epilepsy Res. 104 (1–2) (2013) 26–34.
[23] R. Lazzara, Antiarrhythmic drugs and torsade de pointes, Eur. Heart J. 14 (suppl_H) (1993) 88–92.
[24] H. Furushima, S. Niwano, M. Chinushi, K. Ohhira, A. Abe, Y. Aizawa, Relation between bradycardia dependent long QT syndrome and QT prolongation by disopyramide in humans, Heart 79 (1) (1998) 56–58.
[25] Y.G. Yap, A.J. Camm, Drug induced QT prolongation and torsades de pointes, Heart 89 (11) (2003) 1363–1372.
[26] A. El Harchi, Y.H. Zhang, L. Hussein, C.E. Dempsey, J.C. Hancox, Molecular

determinants of hERG potassium channel inhibition by disopyramide, J. Mol. Cell. Cardiol. 52 (1) (2012) 185–195.
[27] M.J. Zema, Serum drug concentrations and adverse effects in cardiac patients after administration of a new controlled-release disopyramide preparation, Therapeutic Drug Monitor. 6 (2) (1984) 192–198.
[28] C. Du, Y. Zhang, A. El Harchi, C.E. Dempsey, J.C. Hancox, Ranolazine inhibition of hERG potassium channels: drug-pore interactions and reduced potency against inactivation mutants, J. Mol. Cell. Cardiol. 74 (2014) 220–230.
[29] K.J. Broadley, D.R. Kelly, Muscarinic receptor agonists and antagonists, Molecules 6 (3) (2001) 142–193.
[30] I. Peretto, P. Petrillo, B.P. Imbimbo, Medicinal chemistry and therapeutic potential of muscarinic M3 antagonists, Med. Res. Rev. 29 (6) (2009) 867–902.
[31] M.J. Mirro, A.S. Manalan, J.C. Bailey, A.M. Watanabe, Anticholinergic effects of disopyramide and quinidine on guinea pig myocardium. mediation by direct muscarinic receptor blockade, Circulat. Res. 47 (6) (1980) 855–865.
[32] A. Gomółka, A. Ciesielska, M.Z. Wróbel, A. Chodkowski, J. Kleps, M. Dawidowski, A. Siwek, M. Wolak, K. Stachowicz, A. Sławińska, G. Nowak, G. Satała, A.J. Bojarski, M. Belka, S. Ulenberg, T. Bączek, P. Skowronek, J. Turło, F. Herold, Novel, 4-aryl-pyrido[1,2-c]pyrimidines with dual SSRI and 5-HT1A activity. Part 5, Eur. J. Med. Chem. 98 (2015) 221–236.
[33] Z. Zhou, Q. Gong, B. Ye, Z. Fan, J.C. Makielski, G.A. Robertson, C.T. January, Properties of HERG channels stably expressed in HEK 293 cells studied at physiological temperature, Biophys. J. 74 (1) (1998) 230–241.
[34] T. Stöhr, H.J. Kupferberg, J.P. Stables, D. Choi, R.H. Harris, H. Kohn, N. Walton, H.S. White, Lacosamide, a novel anti-convulsant drug, shows efficacy with a wide safety margin in rodent models for epilepsy, Epilepsy Res. 74 (2) (2007) 147–154.
[35] C.S. Metcalf, P.J. West, K.E. Thomson, S.F. Edwards, M.D. Smith, H.S. White, K.S. Wilcox, Development and pharmacologic characterization of the rat 6 Hz model of partial seizures, Epilepsia 58 (6) (2017) 1073–1084.
[36] A. Matagne, H. Klitgaard, Validation of corneally kindled mice: a sensitive screening model for partial epilepsy in man, Epilepsy Res 31 (1) (1998) 59–71.